AD-A113 189   SYRACUSE UNIV NY DEPT OF ELECTRICAL AND COMPUTER EN--ETC F/G 20/14
ELECTROMAGNETIC TRANSMISSION THROUGH APERTURES IN A CAVITY IN A--ETC(U)
JAN 82 Y LEVIATAN, R F HARRINGTON, J R MAUTZ   F30602-79-C-0011

UNCLASSIFIED   RADC-TR-81-386   NL

END
DATE
FILMED
5 82
DTIC

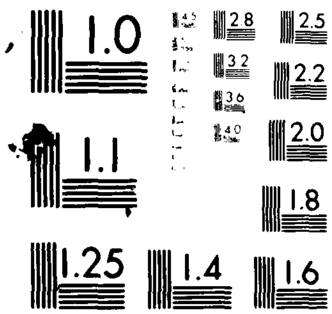

MICROCOPY RESOLUTION TEST CHART

RADC-TR-81-386
Phase Report
January 1982

ELECTROMAGNETIC TRANSMISSION THROUGH APERTURES IN A CAVITY IN A THICK CONDUCTOR

Syracuse University

Yehuda Leviatan
Roger F. Harrington
Joseph R. Mautz

ROME AIR DEVELOPMENT CENTER
Air Force Systems Command
Griffiss Air Force Base, New York 13441

This report has been reviewed by the RADC Public Affairs Office (PA) and is releasable to the National Technical Information Service (NTIS). At NTIS it will be releasable to the general public, including foreign nations.

RADC-TR-81-386 has been revied and is approved for publication.

APPROVED: Roy F. Stratton

ROY F. STRATTON
Project Engineer

APPROVED: David C. Luke

DAVID C. LUKE, Colonel, USAF
Cheif, Reliability & Compatibility Division

FOR THE COMMANDER: John P. Huss

JOHN P. HUSS
Acting Chief, Plans Office

UNCLASSIFIED

SECURITY CLASSIFICATION OF THIS PAGE (When Data Entered)

REPORT DOCUMENTATION PAGE

READ INSTRUCTIONS BEFORE COMPLETING FORM

1. REPORT NUMBER: RADC-TR-81-386	2. GOVT ACCESSION NO.: AD-A113 184
3. RECIPIENT'S CATALOG NUMBER	
4. TITLE (and Subtitle): ELECTROMAGNETIC TRANSMISSION THROUGH APERTURES IN A CAVITY IN A THICK CONDUCTOR	5. TYPE OF REPORT & PERIOD COVERED: Phase Report
	6. PERFORMING ORG. REPORT NUMBER: N/A
7. AUTHOR(s): Yehuda Leviatan, Roger F. Harrington, Joseph R. Mautz	8. CONTRACT OR GRANT NUMBER(s): F30602-79-C-0011
9. PERFORMING ORGANIZATION NAME AND ADDRESS: Syracuse University, Department of Electrical and Computer Engrng., Syracuse NY 13210	10. PROGRAM ELEMENT, PROJECT, TASK AREA & WORK UNIT NUMBERS: 62702F, 23380317
11. CONTROLLING OFFICE NAME AND ADDRESS: Rome Air Development Center (RBCT), Griffiss AFB NY 13441	12. REPORT DATE: January 1982
	13. NUMBER OF PAGES: 66
14. MONITORING AGENCY NAME & ADDRESS (if different from Controlling Office): Same	15. SECURITY CLASS. (of this report): UNCLASSIFIED
	15a. DECLASSIFICATION/DOWNGRADING SCHEDULE: N/A

16. DISTRIBUTION STATEMENT (of this Report)

Approved for public release; distribution unlimited.

17. DISTRIBUTION STATEMENT (of the abstract entered in Block 20, if different from Report)

Same

18. SUPPLEMENTARY NOTES

RADC Project Engineer: Roy F. Stratton (RBCT)

19. KEY WORDS (Continue on reverse side if necessary and identify by block number)

Apertures
Cavity-backed Apertures
Bethe-hole Theory
Thick Conductor
Transmission Through Apertures
Transmission Cross Section
Method of Momen
Equivalent Circ

20. ABSTRACT (Continue on reverse side if necessary and identify by block number)

The general problem of electromagnetic coupling from one region to another through an aperture to cavity to aperture system is specialized to the case of electrically small circular apertures in a cylindrical cavity of circular cross section. A simple equivalent circuit for the coupling system is developed. It is found that for certain cavity depths an exceptionally large amount of electromagnetic energy can be transmitted, and that for identical apertures the transmission cross section of the

system is independent of the size of the apertures.

TABLE OF CONTENTS

LIST OF ILLUSTRATIONS

I. INTRODUCTION

The coupling of electromagnetic energy from one region to another is an important problem in many areas of electromagnetic engineering. Some examples are leakage from microwave ovens, electromagnetic penetration into vehicles, and electromagnetic pulse interaction with shielded electronic equipment.

Our approach is to first obtain the functional equations for the general aperture to cavity to aperture coupling system using the equivalence principle [1, Sec.3-5] and then to reduce these equations to a matrix form via the method of moments [2]. The various matrices are interpreted in terms of generalized network parameters, such as voltages, currents and admittances [2,3]. The formulation of the general problem is similar to the formulation of Auckland and Harrington, who solved for coupling through narrow slots in thick conducting screens [4].

Subsequently the problem is specialized to the case of electrically small circular apertures in a cylindrical cavity of circular cross section and it is assumed that the excitation is due to a plane wave transverse electromagnetic (TEM) to the cylinder axis. The aperture admittances are obtained using the concept of polarizability of apertures developed by Bethe [5,6], and the radiation terms introduced by Harrington [7]. In general an electrically small aperture can be described in terms of a moment solution, where at least three expansion functions must be used to express the equivalent magnetic current. However, for simplicity, we assume that symmetry is such that one expansion function will suffice.

The cavity region can be viewed as a short circuited cylindrical waveguide [8]. Thus waveguide theory can be applied and the field in this region expanded in terms of circular waveguide modes. Furthermore, we assume that all waveguide modes except the dominant TE_{11} mode are in the cutoff condition, thereby obtaining relatively simple formulas and a simple equivalent circuit for the coupling problem.

Special attention has been paid to the case of TE (transverse electric to the cylinder axis) oblique incidence upon the structure and to the effects of cavity losses, both lossy material filling the cavity and finite conductivity of the cylindrical conductor, on the transmission coefficient.

Finally, our discussion is extended and we assume that two waveguide modes, namely, the TE_{11} and the TM_{11}, propagate. TM_{01}, TE_{21}, and TE_{01} modes can propagate but are not excited.

II. FORMULATION OF THE PROBLEM

The problem to be considered is that of coupling between two half-space regions through a cylindrical cavity. Fig. 1 illustrates the cross section of the geometry of the problem. The left-hand half space ($z < 0$) is called region a, the circular cavity region ($0 < \rho < a$, $0 < z < d$) is called region b, and the right-hand half space ($z > d$) is called region c. A circular cavity is a cylindrical cavity of circular cross section. The boundary common to regions a and b is called the aperture A_1. The boundary common to regions b and c is called the aperture A_2. Regions a,b, and c are each filled with homogeneous media of constitutive parameters (μ_a, ε_a), (μ_b, ε_b),and (μ_c, ε_c), respectively. We are not considering dissipation and therefore each μ and each ε is real. The excitation is due to known sources $\underline{J}^i$ and $\underline{M}^i$, with $\exp(j\omega t)$ time dependence, in region a.

The equivalence principle [1, Sec. 3-5] is used to divide the original problem into three equivalent problems, as shown in Figs. 2-4. In region a, the field is produced by the original sources $\underline{J}^i$, $\underline{M}^i$, plus the equivalent magnetic current $-\underline{M}_1$, where

$$\underline{M}_1 = \hat{\underline{n}}_a \times \underline{E} \tag{1}$$

over the aperture region A_1, all radiating in the presence of a complete conductor (aperture A_1 shorted). In (1), $\hat{\underline{n}}_a$ is a unit vector normal to A_1, and $\underline{E}$ is the electric field in the aperture A_1 in the original problem. In region b, the field is produced by the equivalent currents $\underline{M}_1$, given by (1) over A_1, and $-\underline{M}_2$, where

$$\underline{M}_2 = \underline{E} \times \hat{\underline{n}}_c \tag{2}$$

over the aperture region A_2, both radiating in the presence of a conductor completely enclosing the cylindrical cavity region b (both apertures shorted). In (2), the unit vector $\hat{\underline{n}}_c$ is normal to A_2, and $\underline{E}$ is the electric field in the aperture A_2 in the original problem. Finally, in region c we

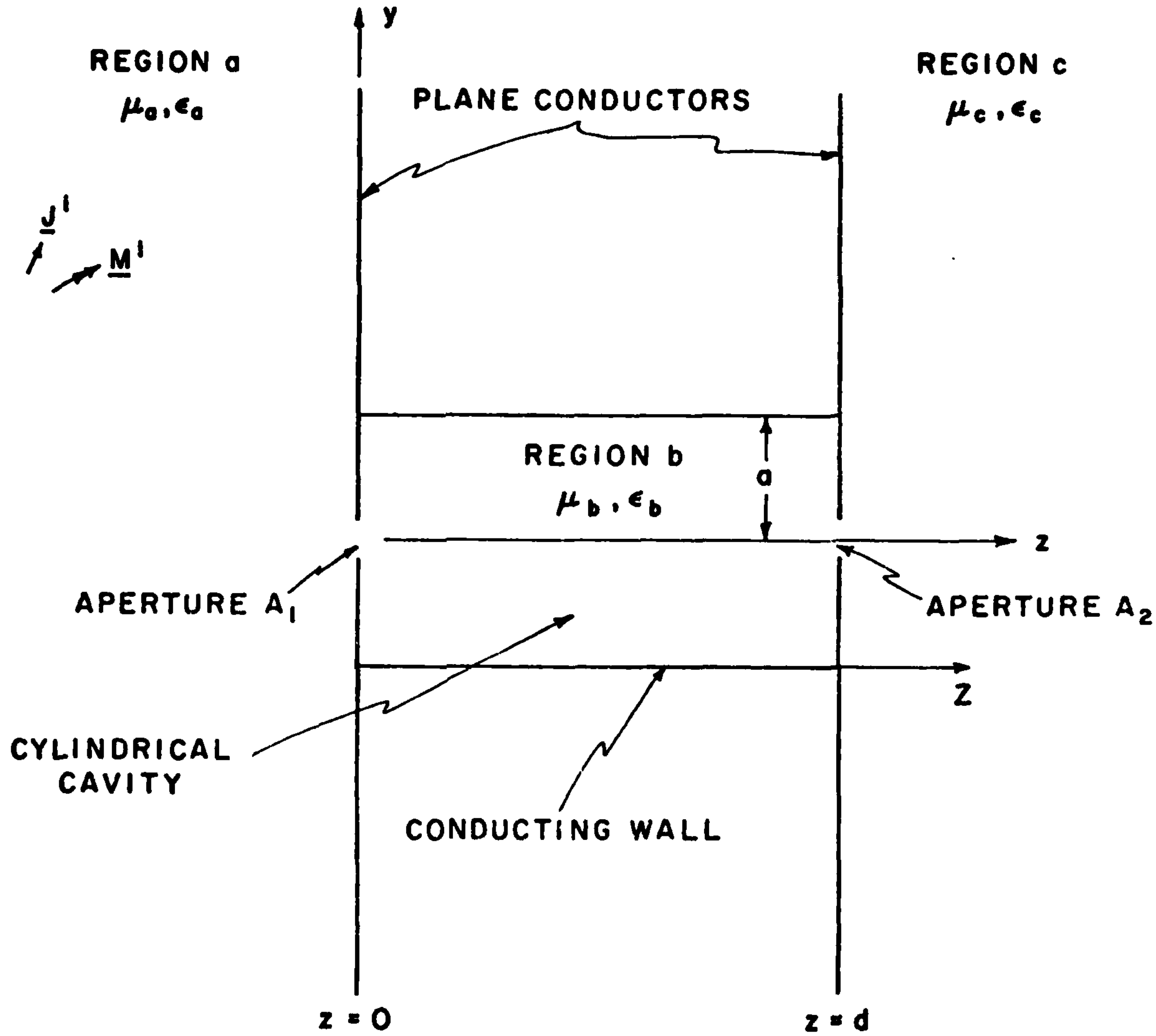

Fig. 1. Geometry of the coupling problem between two half-space regions through a circular cavity.

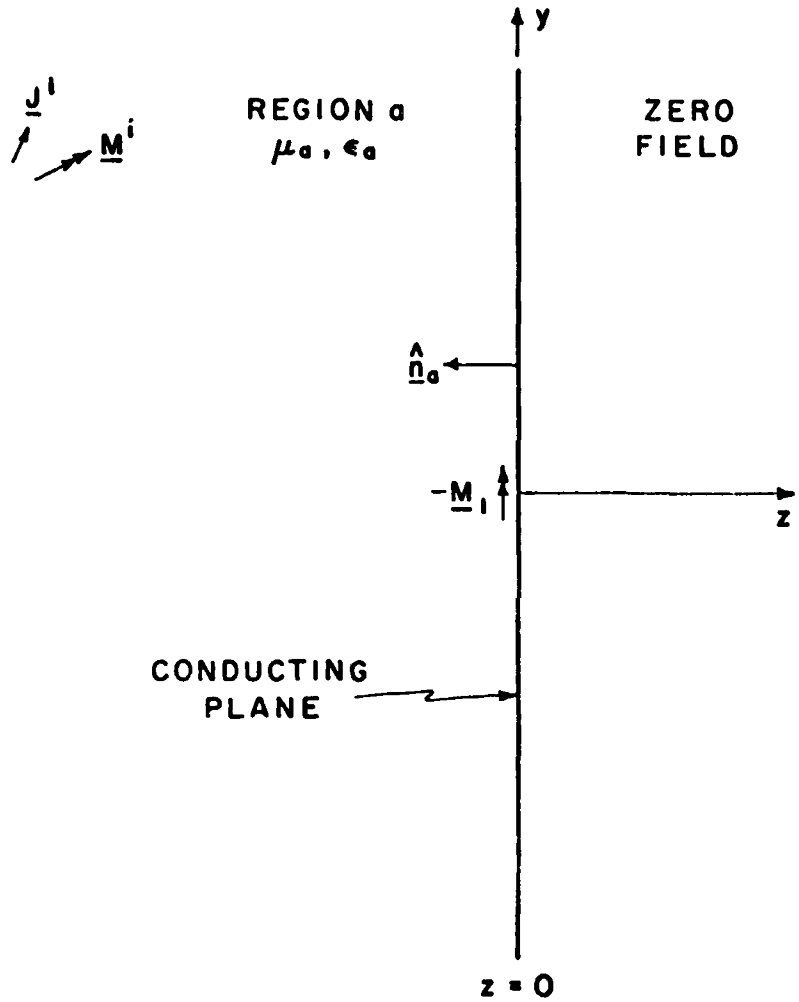

Fig. 2. Equivalence for region a.

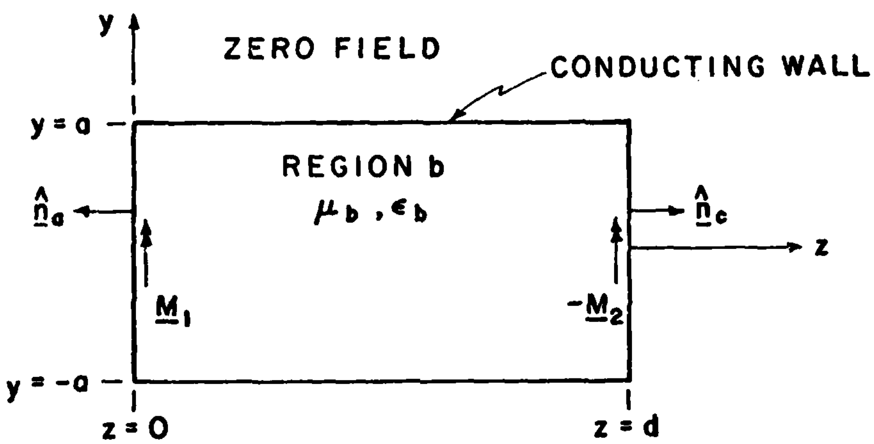

Fig. 3. Equivalence for region b.

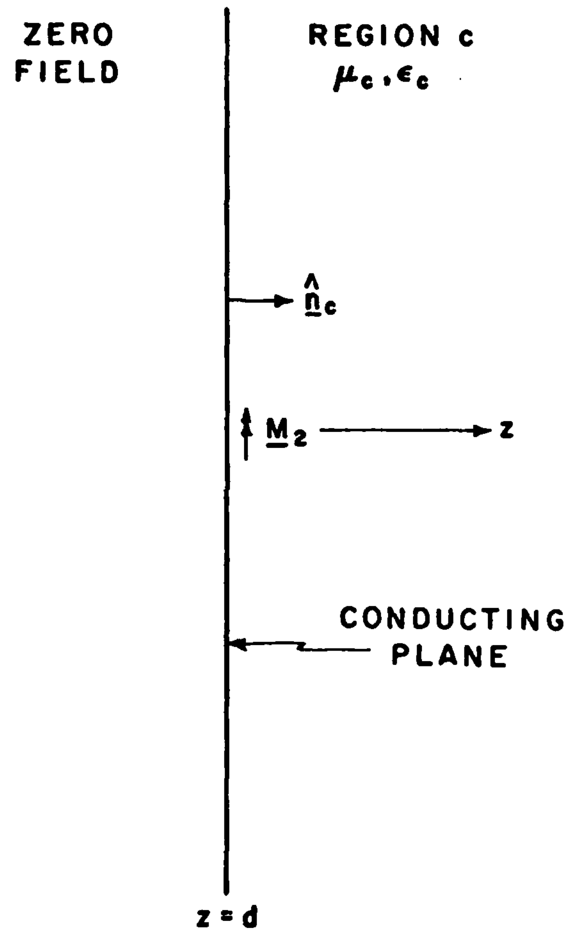

Fig. 4. Equivalence for region c.

have the equivalent magnetic current $\underline{M}_2$ given by (2) over the aperture region A_2, radiating in the presence of a complete conducting plane (aperture A_2 shorted).

The use of $-\underline{M}_1$ in region a and $\underline{M}_1$ in region b ensures continuity of the tangential components of the electric field across the aperture A_1. The use of $-\underline{M}_2$ in region b and $\underline{M}_2$ in region c ensures continuity of the tangential components of the electric field across the aperture A_2. Continuity of the tangential components of $\underline{H}$ across each aperture leads to the operator equations for the problem. The procedure is described in detail in [3]. The result is

$$\begin{aligned} -\underline{H}_t^a(\underline{M}_1) - \underline{H}_t^b(\underline{M}_1) + \underline{H}_t^b(\underline{M}_2) &= -\underline{H}_t^{sc} \qquad \text{over } A_1 \\ \underline{H}_t^b(\underline{M}_1) - \underline{H}_t^b(\underline{M}_2) - \underline{H}_t^c(\underline{M}_2) &= \underline{0} \qquad \text{over } A_2 \end{aligned} \tag{3}$$

where $\underline{H}_t^p(\underline{M}_q)$ denotes the tangential component of $\underline{H}$ due to $\underline{M}_q$ radiating in region p with all apertures shorted, and $\underline{H}_t^{sc}$ denotes the tangential component of $\underline{H}$ due to the impressed sources $\underline{J}^i$, M^i in region a with aperture A_1 shorted. Equation (3) is first solved for the equivalent magnetic currents $\underline{M}_1$ and $\underline{M}_2$, and then the fields in each region can be computed from these equivalent currents.

To obtain a solution to (3), it is convenient to use the method of moments [2]. The procedure is described in detail in [3]. The result can be summarized as follows: Sets of expansion functions $\{\underline{M}_{1n}\}$ in A_1 and $\{\underline{M}_{2n}\}$ in A_2 are assumed, and the equivalent currents are expressed as

$$\begin{aligned} \underline{M}_1 &= \sum_{n=1}^{N_1} V_{1n}\underline{M}_{1n} \\ \underline{M}_2 &= \sum_{n=1}^{N_2} V_{2n}\underline{M}_{2n} \end{aligned} \tag{4}$$

and substituted into (3). Symmetric products

$$< \underline{A}, \underline{B} >_1 = \iint_{A_1} \underline{A} \cdot \underline{B} \, ds$$

$$< \underline{C}, \underline{D} >_2 = \iint_{A_2} \underline{C} \cdot \underline{D} \, ds \tag{5}$$

are defined for each aperture. Sets of testing functions $\{\underline{W}_{1n}\}$ in A_1 and $\{\underline{W}_{2n}\}$ in A_2 are defined, and equations (3) are tested with each $\underline{W}_{qm}$, $m = 1,2,\ldots.N_q$. The result is

$$[Y^a_{11}] \vec{V}_1 + [Y^b_{11}] \vec{V}_1 + [Y^b_{12}] \vec{V}_2 = \vec{I}^i$$

$$[Y^b_{21}] \vec{V}_1 + [Y^b_{22}] \vec{V}_2 + [Y^c_{22}] \vec{V}_2 = \vec{0} \tag{6}$$

where

$$[Y^p_{qq}] = [- <\underline{W}_{qm}, \underline{H}^p_t(\underline{M}_{qn})>_q]_{N_q \times N_q}$$

$$[Y^p_{qr}] = [\ <\underline{W}_{qm}, \underline{H}^p_t(\underline{M}_{rn})>_q]_{N_q \times N_r}, \quad q \neq r \tag{7}$$

$$\vec{I}^i = [- <\underline{W}_{1m}, \underline{H}^{sc}_t >_1]_{N_1 \times 1} \tag{8}$$

$$\vec{V}_q = [V_{qn}]_{N_q \times 1} \tag{9}$$

The matrices $[Y^p_{qr}]$ are called the generalized admittances, the vector $\vec{I}^i$ is called the generalized source current, and the vectors $\vec{V}_q$ are called the generalized voltages. A solution of the problem is obtained by solving the matrix equations (6) for $\vec{V}_1$ and $\vec{V}_2$, which determine the equivalent magnetic currents $\underline{M}_1$ and $\underline{M}_2$ by (4). If a Galerkin solution is used, that is, if $\{\underline{W}_{1n}\} = \{\underline{M}_{1n}\}$ and $\{\underline{W}_{2n}\} = \{\underline{M}_{2n}\}$ it then follows from (7) and (8) that

$$[Y^p_{qq}] = [- \langle \underline{M}_{qm}, \underline{H}^p_t(\underline{M}_{qn}) \rangle_q]_{N_q \times N_q}$$

$$[Y^p_{qr}] = [\ \langle \underline{M}_{qm}, \underline{H}^p_t(\underline{M}_{rn}) \rangle_q]_{N_q \times N_r}, \ q \neq r \tag{10}$$

$$\vec{I}^i = [\ - \langle \underline{M}_{1m}, \underline{H}^{sc}_t \rangle_1]_{N_1 \times 1} \tag{11}$$

It is important to note that computation of $[Y^a_{11}]$ involves only region a , computation of $[Y^b_{11}]$, $[Y^b_{12}]$, $[Y^b_{21}]$, and $[Y^b_{22}]$ involves only region b, and computation of $[Y^c_{22}]$ involves only region c. Hence, we have divided the problem into three parts, each of which may be formulated independently, and therefore we can use previous computations of problems having one of these parts in common. For example, the aperture admittances of electrically small holes for radiation into half-space will be used in the computation of $[Y^a_{11}]$ and $[Y^c_{22}]$.

III. SPECIALIZATION TO SMALL APERTURES, TEM EXCITATION, AND ONE PROPAGATING MODE IN THE CAVITY

The problem is shown in Fig. 5. It is specialized to electrically small circular apertures, of radii R_1 and R_2. Furthermore, it is assumed that only one expansion function each is required for M_1 and M_2. In general, a small hole will require three expansion functions, two for the magnetic dipole moments, and one for the electric dipole moment [5,6], but for now we shall assume that symmetry is such that one will suffice. The excitation is due to a TEM plane wave, which in the absence of the conducting structure propagates in the z direction.

The impressed magnetic field, in the presence of a complete conducting plane over $z = 0$, is taken to be

$$H^{sc}(z) = u_y 2H_o \cos k_a z \tag{12}$$

where H_o is the amplitude of the incident magnetic field, u_y is a unit vector in the y direction and k_a is the wavenumber of medium a. For a small circular aperture, this excites only the y-directed magnetic dipole mode of the aperture A_1. Hence, we let

$$M_1 = V_{11} M_{11} \tag{13}$$

where M_{11} is the quasi static current which produces the effect of a unit magnetic dipole $K\ell = 1$ in the y direction, and V_{11} is a coefficient to be determined. Consequently, the excitation vector, Eq. (11), reduces to the scalar

$$I^i = -H_y^{sc}(0) = -2H_o \tag{14}$$

In region a, one has the half space problem identical to that treated in reference [illegible]. For the above excitation the aperture admittance

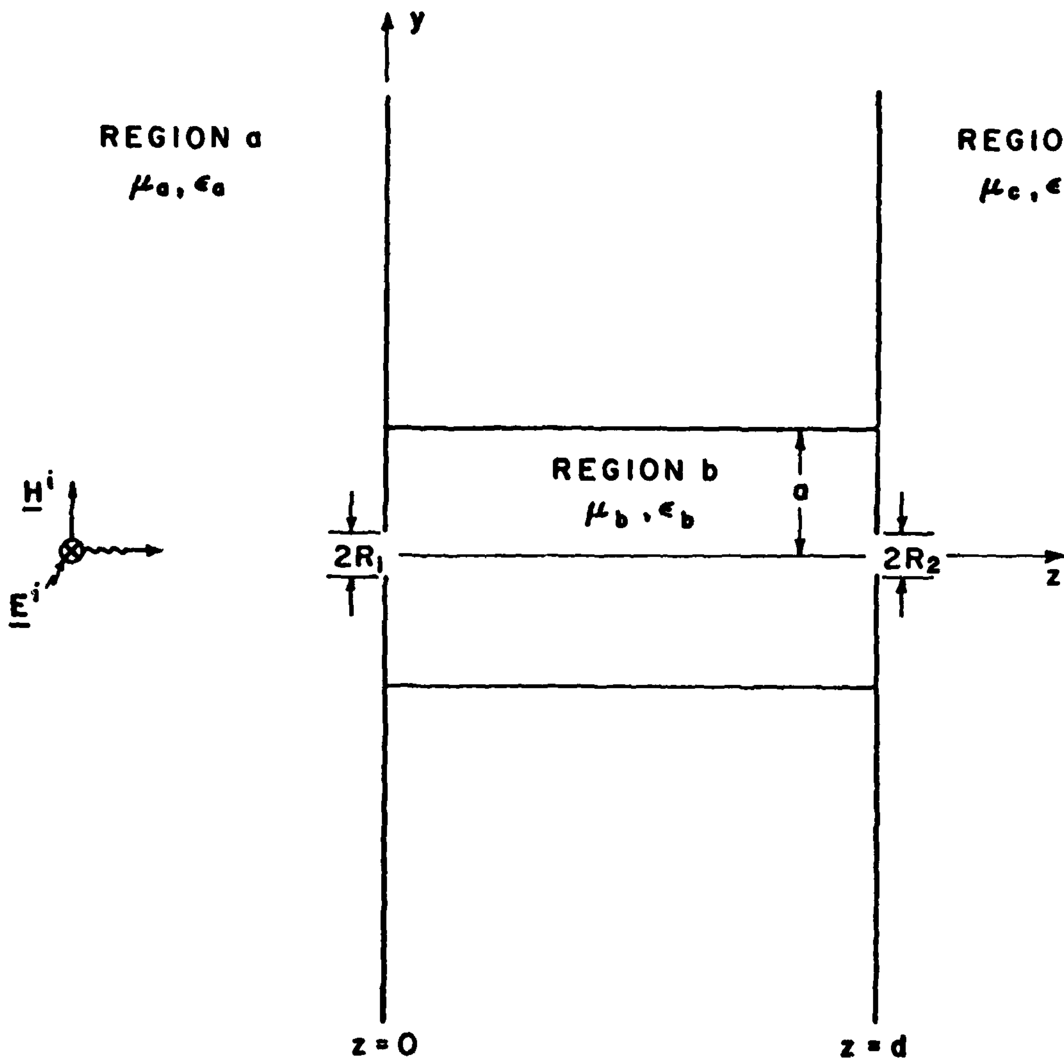

Fig. 5. Gaometry of the coupling problem between two half-space regions through small circular holes in a circular cavity, excited by a plane wave.

reduces to the single element

$$Y_{11}^{a} = \frac{1}{2j\omega\mu_a\alpha_{m1}} + \frac{4\pi}{3\eta_a\lambda_a^2} \tag{15}$$

where α_{m1} is the y-directed magnetic polarizability of a circular aperture related to its radius R_1 by [9]

$$\alpha_{m1} = \frac{4}{3}R_1^3 \tag{16}$$

and μ_a, η_a, and λ_a are the permeability, intrinsic impedance, and wavelength of medium a, respectively.

In region b, the cavity part of the problem, $\underline{M}_1$ excites the TE and TM circular waveguide modes having a modal magnetic vector with nonzero y component at the cylinder axis. The modes excited by $\underline{M}_1$ are the TE_{1p} and TM_{1p} for all p. These modes will excite only the y-directed magnetic dipole mode of the aperture A_2. Hence we let

$$\underline{M}_2 = V_{21}\underline{M}_{21} \tag{17}$$

where $\underline{M}_{21}$ is the quasi-static current which produces the effect of a unit magnetic dipole $K\ell = 1$ in the y direction, and V_{21} is a complex coefficient to be determined.

The transverse (to z) components of the electric and magnetic fields due to $\underline{M}_{r1}$ are called $\underline{E}_t(\underline{M}_{r1})$ and $\underline{H}_t(\underline{M}_{r1})$, respectively, and are expanded in terms of waveguide modes as [1, Sec. 8-1] and [8]

$$\underline{E}_t(\underline{M}_{r1}) = \sum_i V_{r1i}(z)\, \underline{e}_i \tag{18}$$

and

$$\underline{H}_t(\underline{M}_{r1}) = \sum_i I_{r1i}(z)\, \underline{h}_i \tag{19}$$

Here $\underline{e}_i$ and $\underline{h}_i$ are the normalized modal electric and magnetic field vectors and $V_{r1i}(z)$ and $I_{r1i}(z)$ are the modal voltages and currents due to $\underline{M}_{r1}$ only, calculated for the equivalent problem. The summations in (18) and (19) are assumed to be over all modes, both TE and TM if necessary. The total transverse (to z) electric and magnetic fields are then given, respectively, by

$$\underline{E}_t = V_{11}\underline{E}_t(\underline{M}_{11}) - V_{21}\underline{E}_t(\underline{M}_{21}) \tag{20}$$

and

$$\underline{H}_t = V_{11}\underline{H}_t(\underline{M}_{11}) - V_{21}\underline{H}_t(\underline{M}_{21}) \tag{21}$$

In the one-term Galerkin solution, the cavity matrix of admittances becomes

$$\begin{bmatrix} Y^b_{11} & Y^b_{12} \\ Y^b_{21} & Y^b_{22} \end{bmatrix} = \begin{bmatrix} \sum_i -jV^2_{11i}(0)\ Y_i \cot k_i d & \sum_i -jV_{11i}(0)\ V_{21i}(d)\ Y_i \csc k_i d \\ \sum_i -jV_{11i}(0)\ V_{21i}(d)\ Y_i \csc k_i d & \sum_i -jV^2_{21i}(d)\ Y_i \cot k_i d \end{bmatrix} \tag{22}$$

where Y_i is the ith waveguide mode characteristic admittance, k_i is the ith waveguide mode number, and

$$V_{11i}(0) = -\iint_{\substack{\text{apert}\\ A_1}} \underline{M}_{11} \cdot \underline{h}_i \, ds \tag{23}$$

$$V_{21i}(d) = \iint_{\substack{\text{apert}\\ A_2}} \underline{M}_{21} \cdot \underline{h}_i \, ds \tag{24}$$

If all waveguide modes except the dominant TE_{11} ($i = 1$) mode are in the cutoff condition, then all Y_i and k_i are imaginary except Y_1 and k_1. Note that there are two TE_{11} modes, but only one of them is excited. We let

$$\left.\begin{array}{l} Y_i = jB_i \\ \\ k_i = -j\alpha_i \end{array}\right\} \quad i \neq 1 \tag{25}$$

and the elements of the admittance matrix in (22) become

$$\begin{bmatrix} Y^b_{11} & Y^b_{12} \\ \\ Y^b_{21} & Y^b_{22} \end{bmatrix} = \begin{bmatrix} -jn^2_{11}Y_1 \cot k_1 d + jB_{11} & jn_{11}n_{21}Y_1 \csc k_1 d + jB_{12} \\ \\ jn_{11}n_{21}Y_1 \csc k_1 d + jB_{21} & -jn^2_{21}Y_1 \cot k_1 d + jB_{22} \end{bmatrix} \tag{26}$$

where

$$n_{11} = V_{111}(0), \; n_{21} = -V_{211}(d) \tag{27}$$

$$B_{11} = \sum_{i\neq 1} V^2_{11i}(0) B_i \coth \alpha_i d, \qquad B_{22} = \sum_{i\neq 1} V^2_{21i}(d) B_i \coth \alpha_i d \tag{28}$$

$$B_{12} = B_{21} = \sum_{i\neq 1} V_{11i}(0) \; V_{21i}(d) \, B_i \operatorname{csch} \alpha_i d \tag{29}$$

Whenever $\alpha_i d >> 1$ $(i \neq 1)$, $\operatorname{csch} \alpha_i d \to 0$. Hence, B_{12} and B_{21} may be neglected in Y^b_{12} and Y^b_{21}, respectively. This fact is evident since the fields due to those nonpropagating modes exist primarily in the vicinity of the apertures, and thus their contribution to the coupling between the two apertures is negligible. However, these fields do contribute to the input admittances Y^b_{11} and Y^b_{22} of the two cavity backed apertures. As the sizes of the apertures decrease,the fields become more localized, more modes are required for an adequate respresentation, and the proportionate contribution of each particular mode (such as the $i = 1$ mode) becomes smaller. Therefore, provided the cavity sides are not close to other boundary surfaces, the susceptances B_{11} and B_{22} are essentially the same as the susceptance of an aperture in an infinite plane conducting screen [10]. Hence we let,

$$B_{11} = -\frac{3}{8\omega\mu_b R_1^3}, \quad B_{22} = -\frac{3}{8\omega\mu_b R_2^3}, \quad B_{12} = B_{21} = 0 \tag{30}$$

where μ_b is the permeability of medium b. The matrix of admittances Eq. (26) becomes

$$\begin{bmatrix} Y_{11}^b & Y_{12}^b \\ Y_{21}^b & Y_{22}^b \end{bmatrix} = \begin{bmatrix} -jn_{11}^2 Y_1 \cot k_1 d + jB_{11} & jn_{11}n_{21}Y_1 \csc k_1 d \\ jn_{11}n_{21}Y_1 \csc k_1 d & -jn_{21}^2 Y_1 \cot k_1 d + jB_{22} \end{bmatrix} \tag{31}$$

This is the two-port admittance matrix for a transmission line of length d, having a characteristic admittance Y_1, and a propagation constant k_1, with a shunt susceptance B_{11} connected to its input terminal through an ideal transformer of turns ratio n_{11} and a shunt susçeptance B_{22} connected to its output terminal through an ideal transformer of turns ratio n_{21}. This two-port matrix is the part of the equivalent circuit labeled region b in Fig. 6.

The characterization of region c is similar to that of region a. Hence, one has

$$Y_{22}^c = \frac{3}{j8\omega\mu_c R_2^3} + \frac{4\pi}{3\eta_c \lambda_c^2} \tag{32}$$

where μ_c, η_c, and λ_c are the permeability, intrinsic impedance, and wavelength of medium c, respectively.

Thanks to (31), the equivalent circuit for the one term moment equation (6) is the circuit given in Fig. 6. This circuit may be reduced to the equivalent

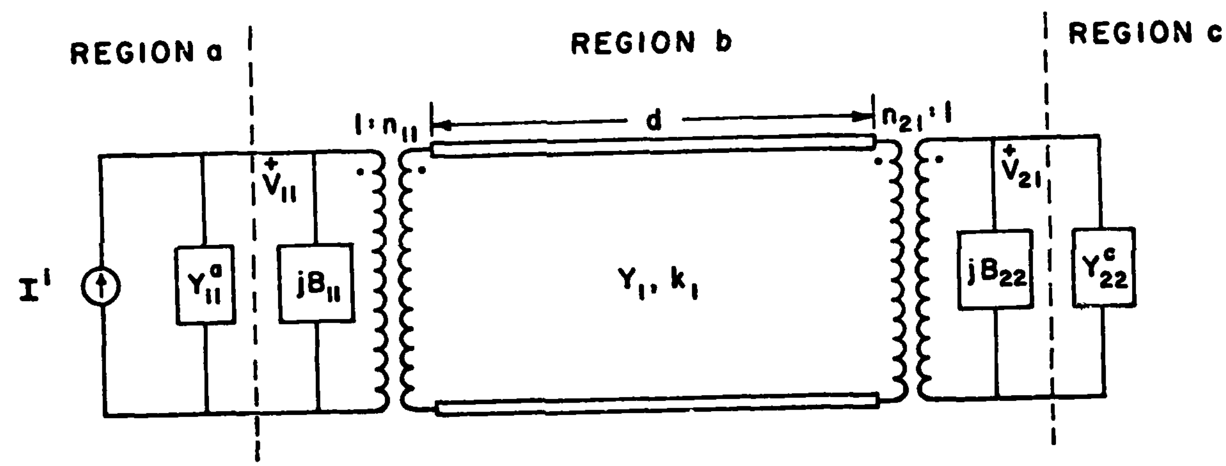

Fig. 6. Equivalent circuit for the coupling between two small circular apertures through a circular cavity, assuming all waveguide modes other than the TE_{11} mode are in the cutoff condition.

circuit of Fig. 7 because

$$\iint_{A_2} \underline{M}_{21} \cdot \underline{h}_1 \, ds \approx \iint_{A_1} \underline{M}_{11} \cdot \underline{h}_1 ds$$

so that for practical considerations we may take

$$n_{21} = n_{11}$$

A parameter of interest is the transfer admittance [4]

$$Y_{12} = \frac{I^i}{V_{21}} = \frac{Y^b_{12}Y^b_{21} - (Y^a_{11} + Y^b_{11})(Y^b_{22} + Y^c_{22})}{Y^b_{21}} \tag{33}$$

which allows one to calculate the strength of $\underline{M}_2 = V_{21}\underline{M}_{21}$, given the excitation I^i of (14). Setting $n_{21} = n_{11}$ in (31) and then substituting (31) into (33), we obtain

$$\begin{aligned} Y_{12} &= [Y^a_{11} + Y^c_{22} + j(B_{11} + B_{22})]\cos k_1 d \\ &+ j[n^2_{11}Y_1 + \frac{(Y^a_{11} + jB_{11})(Y^c_{22} + jB_{22})}{n^2_{11}Y_1}]\sin k_1 d \end{aligned} \tag{34}$$

Equation (34) can also be obtained from the equivalent circuit in Fig. 7. Denoting the aperture admittances by

$$Y^a_{11} = G^a + jB^a \quad \text{and} \quad Y^c_{22} = G^c + jB^c \tag{35}$$

we can write the real and imaginary parts of Y_{12} as given by (34) as

$$\mathrm{Re}(Y_{12}) = (G^a + G^c)\cos k_1 d - \frac{G^a(B^c + B_{22}) + G^c(B^a + B_{11})}{n^2_{11}Y_1} \sin k_1 d \tag{36}$$

$$\begin{aligned} \mathrm{Im}(Y_{12}) &= (B^a + B^c + B_{11} + B_{22})\cos k_1 d \\ &+ [n^2_{11}Y_1 + \frac{G^aG^c - (B^a + B_{11})(B^c + B_{22})}{n^2_{11}Y_1}]\sin k_1 d \end{aligned} \tag{37}$$

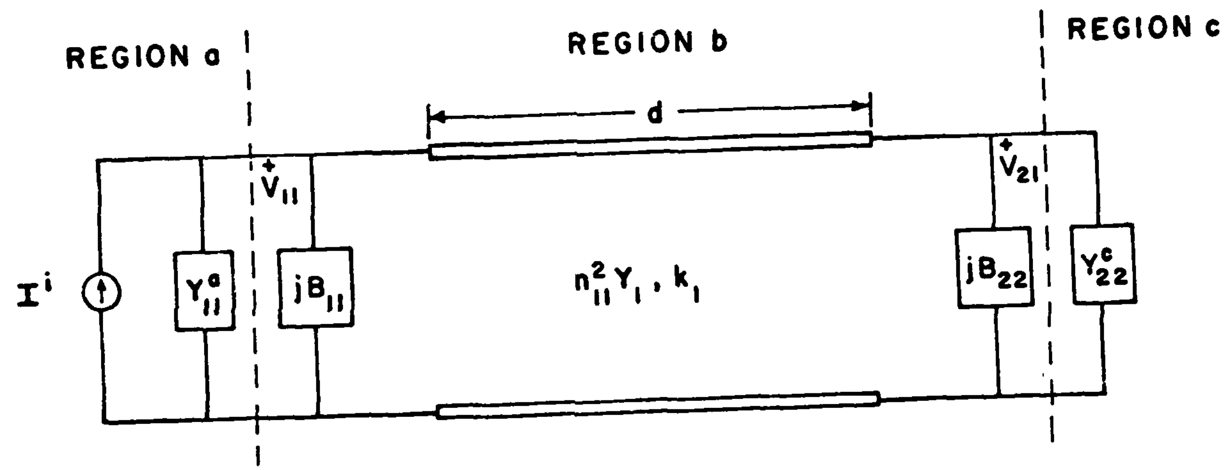

Fig. 7. Reduced representation of the equivalent circuit of Fig. 6 obtained by using $n_{21} = n_{11}$.

To complete our formulation we need to specify the parameters related to the $i = 1$ (TE_{11}) dominant mode of the circular waveguide. The normalized modal magnetic and electric field vectors of the TE_{11} mode in a cylindrical coordinate system are [1, Sec. 8.1]

$$\underline{h}_1 = -0.887\left[\frac{1.841}{a} J_1'\left(\frac{1.841}{a}\rho\right) \sin\phi \, \underline{u}_\rho + \frac{1}{\rho} J_1\left(\frac{1.841}{a}\rho\right) \cos\phi \, \underline{u}_\phi\right] \tag{38}$$

$$\underline{e}_1 = \underline{h}_1 \times \underline{u}_z \tag{39}$$

where $J_1(x)$ is the Bessel function of the first kind of order 1 and $J_1'(x)$ denotes the derivative of $J_1(x)$ with respect to x. The modal wave number is

$$k_1 = \left[\omega^2 \mu_b \varepsilon_b - \left(\frac{1.841}{a}\right)^2\right]^{1/2} \tag{40}$$

and its modal characteristic admittance is

$$Y_1 = \frac{k_1}{\omega\mu_b} \tag{41}$$

Another parameter of interest is the turns ratio n_{11}. Substitution of (38) into (23) yields

$$V_{111}(0) = \frac{0.816}{a} \tag{42}$$

and from (27) one readily obtains

$$n_{11} = \frac{0.816}{a} \tag{43}$$

IV. POWER TRANSMITTED

The power transmitted through the cavity to region c is equal to the power dissipated in Y_{22}^c of the equivalent circuit, that is

$$P_{trans} = |V_{21}|^2 G^c \tag{44}$$

In terms of the transfer admittance (33), this is

$$P_{trans} = \left|\frac{I^i}{Y_{12}}\right|^2 G^c \tag{45}$$

where I^i is given by (14), Y_{12} by (36) and (37), and $G^c = \mathrm{Re}(Y_{22}^c)$. Here, Y_{22}^c is given by (32).

The power incident upon the aperture A_1 when the incidence is normal is

$$P_{inc}^n = \eta_a |H_o|^2 A \tag{46}$$

where H_o is the amplitude of the incident field, and $A = \pi R_1^2$ is the area of the aperture A_1. The superscript n means that the power defined here is for normal incidence. One can define the transmission coefficient T of the cavity to be the power transmitted through the cavity to region c normalized with respect to the incident power (46), that is

$$T = \frac{P_{trans}}{P_{inc}^n} \tag{47}$$

Now, substitution from (14), (45) and (46) into (47) results in

$$T = \frac{4G^c}{\eta_a \, |Y_{12}|^2 \, A} = \frac{16\pi}{3\eta_a \eta_c \, \lambda_c^2 \, |Y_{12}|^2 \, A} \tag{48}$$

The transmission coefficient (48) depends on the cavity depth d only through the parameter Y_{12}. It will attain its maximum when $|Y_{12}|$ is minimum. For small apertures we see that $B^a \gg G^a$ and $B^c \gg G^c$. Hence, the coefficients of the trigonometric terms in (37) are much larger than those in (36), and we can minimize $|Y_{12}|$ by setting $\mathrm{Im}(Y_{12}) = 0$. Doing this and retaining only dominant terms, we obtain

$$\tan k_1 d \simeq \frac{(B^a + B^c + B_{11} + B_{22})}{(B^a + B_{11})(B^c + B_{22})} n_{11}^2 Y_1 \tag{49}$$

Since the right-hand side of Eq. (49) is a small negative number, a first order approximation to resonance is

$$k_1 d \simeq m\pi + \frac{(B^a + B^c + B_{11} + B_{22})}{(B^a + B_{11})(B^c + B_{22})} n_{11}^2 Y_1$$

or

$$d_{res} \simeq [m + \frac{(B^a + B^c + B_{11} + B_{22})}{(B^a + B_{11})(B^c + B_{22})} \frac{n_{11}^2 Y_1}{\pi}] \frac{\lambda_1}{2} \tag{50}$$

Here the subscript "res" denotes "at resonance", λ_1 is the wavelength of the dominant mode in the cavity region, and m = 1, 2, 3.... .

Next we wish to obtain the transmission coefficient at resonance. Using the approximations

$$\cos k_1 d_{res} \simeq (-1)^m$$

$$\sin k_1 d_{res} \simeq (-1)^m \frac{(B^a + B^c + B_{11} + B_{22})}{(B^a + B_{11})(B^c + B_{22})} n_{11}^2 Y_1 \qquad (51)$$

in (36), we obtain

$$Re(Y_{12})_{res} = (-1)^m \left\{ (G^a + G^c) - (B^a + B^c + B_{11} + B_{22}) \left[\frac{G^a}{B^a + B_{11}} + \frac{G^c}{B^c + B_{22}} \right] \right\} \qquad (52)$$

If we introduce the parameters

$$\bar{\mu}_b = \frac{\mu_b}{\mu_a} \quad , \quad \bar{\varepsilon}_b = \frac{\varepsilon_b}{\varepsilon_a}$$

$$\bar{\mu}_c = \frac{\mu_c}{\mu_a} \quad , \quad \bar{\varepsilon}_c = \frac{\varepsilon_c}{\varepsilon_a} \qquad (53)$$

$$\chi = \left(\frac{R_1}{R_2}\right)^3 \qquad (54)$$

we obtain

$$\eta_c = \left(\frac{\bar{\mu}_c}{\bar{\varepsilon}_c}\right)^{1/2} \eta_a \qquad (55)$$

$$\lambda_c = \frac{1}{(\bar{\mu}_c \bar{\varepsilon}_c)^{1/2}} \lambda_a \qquad (56)$$

Now substituting for G^a, B^a, B_{11}, B_{22}, G^c and B^c as obtained from (15), (30) and (32), using the parameters defined in (53) and (54), and applying the relations (55) and (56), we cast (52) into the form

$$\mathrm{Re}(Y_{12})_{res} = (-1)^m \frac{4\pi}{3\eta_a \lambda_a^2} \left\{ 1 + \bar{\varepsilon}_c (\bar{\mu}_c \bar{\varepsilon}_c)^{1/2} \right.$$

$$\left. - [\chi(\bar{\mu}_b + \bar{\mu}_c) + \bar{\mu}_c(1 + \bar{\mu}_b)] [\frac{1}{\bar{\mu}_c(1 + \bar{\mu}_b)} + \frac{\bar{\varepsilon}_c(\bar{\mu}_c\bar{\varepsilon}_c)^{1/2}}{\chi(\bar{\mu}_b + \bar{\mu}_c)}] \right\} \tag{57}$$

At resonance, (48) can be written as

$$T_{res} = \frac{16\pi\, \bar{\varepsilon}_c (\bar{\mu}_c \bar{\varepsilon}_c)^{1/2}}{3\, \eta_a^2\, \lambda_a^2\, |\mathrm{Re}(Y_{12})_{res}|^2\, A} \tag{58}$$

and (50) as

$$d_{res} \simeq [m - 3.556 \frac{\chi(\bar{\mu}_b + \bar{\mu}_c) + \bar{\mu}_c(1 + \bar{\mu}_b)}{(1 + \bar{\mu}_b)(\bar{\mu}_b + \bar{\mu}_c)} \frac{R_2^3}{a^2 \lambda_1}] \frac{\lambda_1}{2} \tag{59}$$

If medium a, medium b, and medium c are the same (i.e., $\bar{\mu}_b = \bar{\mu}_c = \bar{\varepsilon}_c = 1$) and if $R_1 = R_2$ (i.e., $\chi = 1$), (57) reduces to

$$\mathrm{Re}\ (Y_{12})_{res} = (-1)^{m+1} \frac{8\pi}{3\eta_a\ \lambda_a^2} \tag{60}$$

The resonance occurs at

$$d_{res} \simeq [m - 3.556 \frac{R_1^3}{\lambda_1 a^2}] \frac{\lambda_1}{2} \tag{61}$$

and the transmission coefficient at resonance (58) becomes

$$T_{res} = \frac{3\lambda_a^2}{4\pi A} \tag{62}$$

The transmission cross section of the system is defined as the area for which the incident wave contains the power transmitted by the system. It follows that the transmission cross section is equal to TA. From (48), one obtains

$$TA = \frac{4G^c}{\eta_a |Y_{12}|^2} = \frac{16\pi}{3\eta_a \eta_c \lambda_c^2 |Y_{12}|^2} \tag{63}$$

If media a, b, and c are the same, one obtains from (62) that the transmission cross section at resonance becomes $(TA)_{res} = 3\lambda_a^2/4\pi$ independent of the common radius $R_1 = R_2$ of the apertures. This transmission cross section and the transmission coefficient (62) are the same as those obtained in [7] for a small slot in a zero-thickness plane conducting screen, resonated by a capacitor placed across its midpoint, and excited by an incident electric field perpendicular to its axis.

V. OBLIQUE INCIDENCE UPON THE STRUCTURE (TE CASE), AND ONE PROPAGATING MODE IN THE CAVITY

Consider a plane wave incident upon the structure at some angle θ_{inc} in the y-z plane measured from the negative z axis, as shown in Fig. 8. This is a TE (transverse electric to the cylinder axis) excitation. Following an approach similar to that of section III, we reduce the excitation vector, Eq. (11), to the scalar

$$I^{i} = -H_{y}^{sc}(0) = -2H_{o} \cos \theta_{inc} \tag{64}$$

where H_o is the amplitude of the incident magnetic field.

Except for the fact that I^i is now given by (64) instead of (14), the equivalent circuit and its parameters remain unchanged. The power transmitted through the cavity to region c is given by (44), and in terms of the transfer admittance by (45). Substitution of I^i from (64) into (45) results in

$$P_{trans} = \frac{4|H_o|^2 \cos^2 \theta_{inc}}{|Y_{12}|^2} G^c \tag{65}$$

where Y_{12} is given by (36) and (37) and $G^c = \mathrm{Re}(Y_{22}^c)$ with Y_{22}^c given by (32).

The transmission coefficient is defined by Eq. (47). Substituting from (65) and (46) into (47), one obtains

$$T = \frac{4G^c}{\eta_a |Y_{12}|^2 A} \cos^2 \theta_{inc} = \frac{16\pi}{3\eta_a \eta_c \lambda_c |Y_{12}|^2 A} \cos^2 \theta_{inc} \tag{66}$$

Note that here P_{inc}, the actual power incident upon the aperture A_1, is related to the power P_{inc}^n given by (46) by

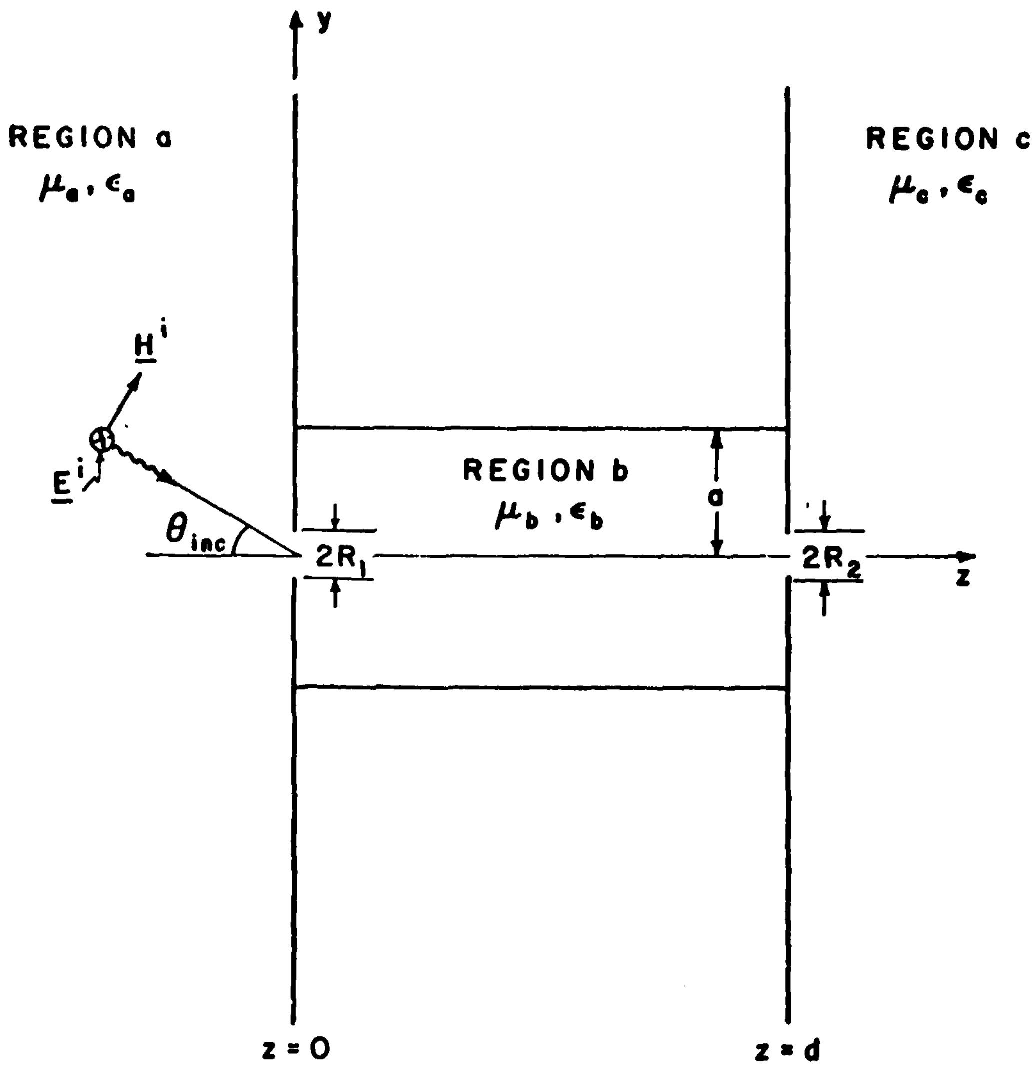

Fig. 8. TE oblique incidence upon the structure.

$$P_{inc} = P_{inc}^{n} \cos\theta_{inc} \tag{67}$$

Eq.(66) reduces, as expected, to (48) for normal incidence ($\theta_{inc} = 0^{o}$).

VI. THE EFFECT OF CAVITY LOSSES

The previous formulation may be extended to encompass the effects of lossy material filling the cavity and of imperfect conductivity of the circular walls of the cavity. The previous equivalent circuit still holds except that the modal wave number of the circular waveguide dominant mode is changed from purely real to complex with a small imaginary part ($k_1 = k_1' - jk_1''$). Nevertheless, the following two simplifying assumptions can be made: (a) The characteristic admittance Y_1 can still be considered real, and (b) the real part of the modal wave number is equal to the wave number of the mode in the loss-free case. These assumptions are certainly valid for the low-loss cavity. The imaginary part of the wave number k_1'' may be cast into the form

$$k_1'' = \alpha_d + \alpha_c \tag{68}$$

where α_d is the attenuation constant due to lossy dielectric ($\varepsilon_b = \varepsilon_b' - j\varepsilon_b''$)

$$\alpha_d = \frac{\omega\varepsilon_b''}{2} \eta_b \left[1 - \left(\frac{1.841}{k_b a}\right)^2\right]^{-1/2} \tag{69}$$

and α_c is the attenuation constant due to imperfect conductor

$$\alpha_c = \frac{R_s}{a\eta_b} \left[1 - \left(\frac{1.841}{k_b a}\right)^2\right]^{-1/2} \left[\left(\frac{1.841}{k_b a}\right)^2 + \frac{1}{(1.841)^2 - 1}\right] \tag{70}$$

Here, $\eta_b = (\mu_b/\varepsilon_b')^{1/2}$, $k_b = \omega(\mu_b\varepsilon_b')^{1/2}$, and $R_s = (\frac{\omega\mu}{2\sigma})^{1/2}$ is the surface resistance due to finite conductivity σ.

The expected effects of lossy dielectric filling the cavity are smaller transmitted power and broader resonance curves. Similar effects are expected if the circular conductor has finite but small conductivity. Equating the attenuation constants of (69) and (70), we obtain that a lossy conductor case behaves like a lossy dielectric case ($\varepsilon_b = \varepsilon_b' - j\varepsilon_b''$ and quality factor $Q_d = \varepsilon_b'/\varepsilon_b''$) if the quality factor due to conductor losses, defined as,

$$Q_c = \frac{k_b \eta_b a}{2R_s} \frac{1}{\left[\left(\frac{1.841}{k_b a}\right)^2 + \frac{1}{(1.841)^2 - 1}\right]} \tag{71}$$

is equal to the quality factor due to dielectric losses Q_d.

VII. TWO PROPAGATING MODES IN THE CAVITY (TEM AND TE EXCITATIONS)

The problems to be considered are the problems of Fig. 5 (TEM excitation) and of Fig. 8 (TE excitation) treated in sections III and V, respectively. Here we extend our discussion and assume that two excited waveguide modes, namely, the TE_{11} and the TM_{11}, propagate. The differences appear in the admittance representation of the cavity region. The parameters of the equivalent circuits for region a and region c remain unchanged, and may be extracted from sections III and V for the TEM and TE excitations, respectively.

If all excited waveguide modes except the TE_{11} (i = 1) and TM_{11} (i = 2) modes are in the cutoff condition, then all Y_i and k_i are imaginary except Y_1, k_1 , Y_2, and k_2. We let

$$\left.\begin{aligned} Y_i &= jB_i \\ k_i &= -j\alpha_i \end{aligned}\right\} \quad i \neq 1,2 \tag{72}$$

and the elements of the admittance matrix in (22) become

$$\begin{bmatrix} Y^b_{11} & Y^b_{12} \\ Y^b_{21} & Y^b_{22} \end{bmatrix} = \begin{bmatrix} \begin{matrix} -jV^2_{111}(0)Y_1 \cot k_1d \\ -jV^2_{112}(0)Y_2 \cot k_2d + jB'_{11} \end{matrix} & \begin{matrix} -jV_{111}(0)V_{211}(d)Y_1 \csc k_1d \\ -jV_{112}(0)V_{212}(d)Y_2 \csc k_2d + jB'_{12} \end{matrix} \\ \begin{matrix} -jV_{111}(0)V_{211}(d)Y_1 \csc k_1d \\ -jV_{112}(0)V_{212}(d)Y_2 \csc k_2d + jB'_{21} \end{matrix} & \begin{matrix} -jV^2_{211}(d)Y_1 \cot k_1d \\ -jV^2_{212}(d)Y_2 \cot k_2d + jB'_{22} \end{matrix} \end{bmatrix} \tag{73}$$

where

$$B'_{11} = \sum_{i\neq 1,2} V^2_{11i}(0)B_i \coth \alpha_i d; \quad B'_{22} = \sum_{i\neq 1,2} V^2_{21i}(d)B_i \coth \alpha_i d \qquad (74)$$

$$B'_{12} = B'_{21} = \sum_{i\neq 1,2} V_{11i}(0)\ V_{21i}(d)B_i \operatorname{csch} \alpha_i d \qquad (75)$$

Whenever $\alpha_i d >> 1$ $(i \neq 1,2)$, B'_{12} and B'_{21} may be neglected in Y^b_{12} and Y^b_{21}, respectively. Using an argument similar to that of section III, we conclude again that B'_{11} and B'_{22} are essentially the same as the susceptance of an aperture in an infinite plane conducting screen. Thus

$$B'_{11} = -\frac{3}{8\omega\mu_b R_1^3}\ ; \quad B'_{22} = -\frac{3}{8\omega\mu_b R_2^3} \qquad (76)$$

Now, the matrix of admittances (73) becomes

$$\begin{bmatrix} Y^b_{11} & Y^b_{12} \\ Y^b_{21} & Y^b_{22} \end{bmatrix} = \begin{bmatrix} -jn^2_{11}Y_1 \cot k_1 d \ -jn^2_{12}Y_2 \cot k_2 d + jB'_{11} & jn_{11}n_{21}Y_1 \csc k_1 d + jn_{12}n_{22}Y_2 \csc k_2 d \\ jn_{11}n_{21}Y_1 \csc k_1 d + jn_{12}n_{22}Y_2 \csc k_2 d & -jn^2_{21}Y_1 \cot k_1 d - jn^2_{22}Y_2 \cot k_2 d + jB'_{22} \end{bmatrix} \qquad (77)$$

where

$$\begin{aligned} n_{11} &= V_{111}(0) \\ n_{12} &= V_{112}(0) \\ n_{21} &= -V_{211}(d) \\ n_{22} &= -V_{212}(d) \end{aligned} \qquad (78)$$

This is the two-port admittance matrix for two transmission lines of length d, having characteristic admittances Y_1 and Y_2, respectively, and propagation constants k_1 and k_2, respectively, with shunt susceptances B'_{11} and B'_{22}

connected through ideal transformers, at their input and output ports.

The equivalent circuit for this one term moment solution is given in Fig. 9, and it may be reduced to the equivalent circuit of Fig. 10. This last step is due to the fact that for the propagating modes we have

$$\iint_{A_1} \underline{M}_{11} \cdot \underline{h}_1 \, ds \simeq \iint_{A_2} \underline{M}_{21} \cdot \underline{h}_1 \, ds$$

and

$$\iint_{A_1} \underline{M}_{11} \cdot \underline{h}_2 \, ds \simeq \iint_{A_2} \underline{M}_{21} \cdot \underline{h}_2 \, ds.$$

Therefore, for practical considerations, we may take $n_{21} = n_{11}$ and $n_{22} = n_{12}$.

The transfer admittance, Y_{12}, defined by Eq. (33) is obtained from Fig. 10. That is,

$$\begin{aligned} Y_{12} = \Big\{ & [Y^a_{11} + Y^c_{22} + j(B'_{11} + B'_{22})][n^2_{11}Y_1 \cos k_1d \sin k_2d + n^2_{12}Y_2 \cos k_2d \sin k_1d] \\ & + j[(n^2_{11}Y_1)^2 + (n^2_{12}Y_2)^2 + (Y^a_{11} + jB'_{11})(Y^c_{22} + jB'_{22})]\sin k_1d \sin k_2d \\ & + 2jn^2_{11}n^2_{12}Y_1Y_2[1 - \cos k_1d \cos k_2d]\Big\} \; [n^2_{11}Y_1 \sin k_2d + n^2_{12}Y_2 \sin k_1d]^{-1} \end{aligned} \tag{79}$$

Once the transfer admittance is obtained from (79) the transmission coefficient may be computed from (48) and (66) for normal and oblique incidence, respectively.

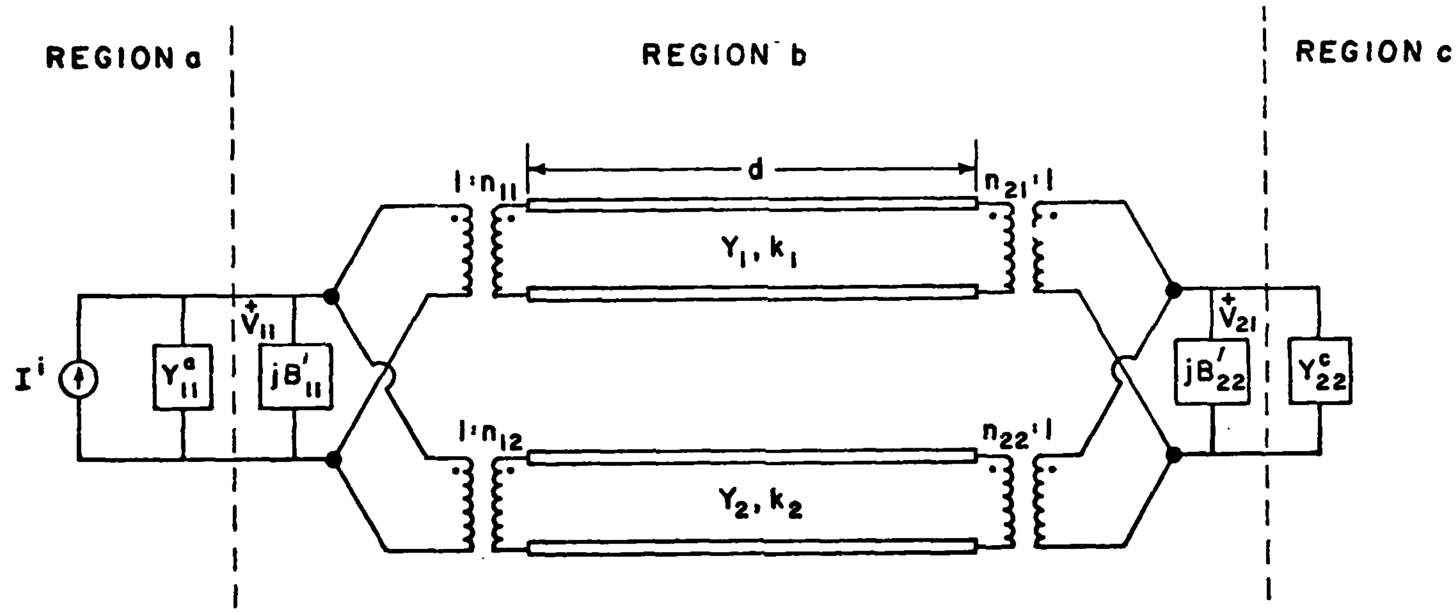

Fig. 9. Equivalent circuit for the coupling between two small circular apertures through a circular cavity in case of TE excitation, assuming all waveguide modes except the TE_{11} and TM_{11} modes are not propagating.

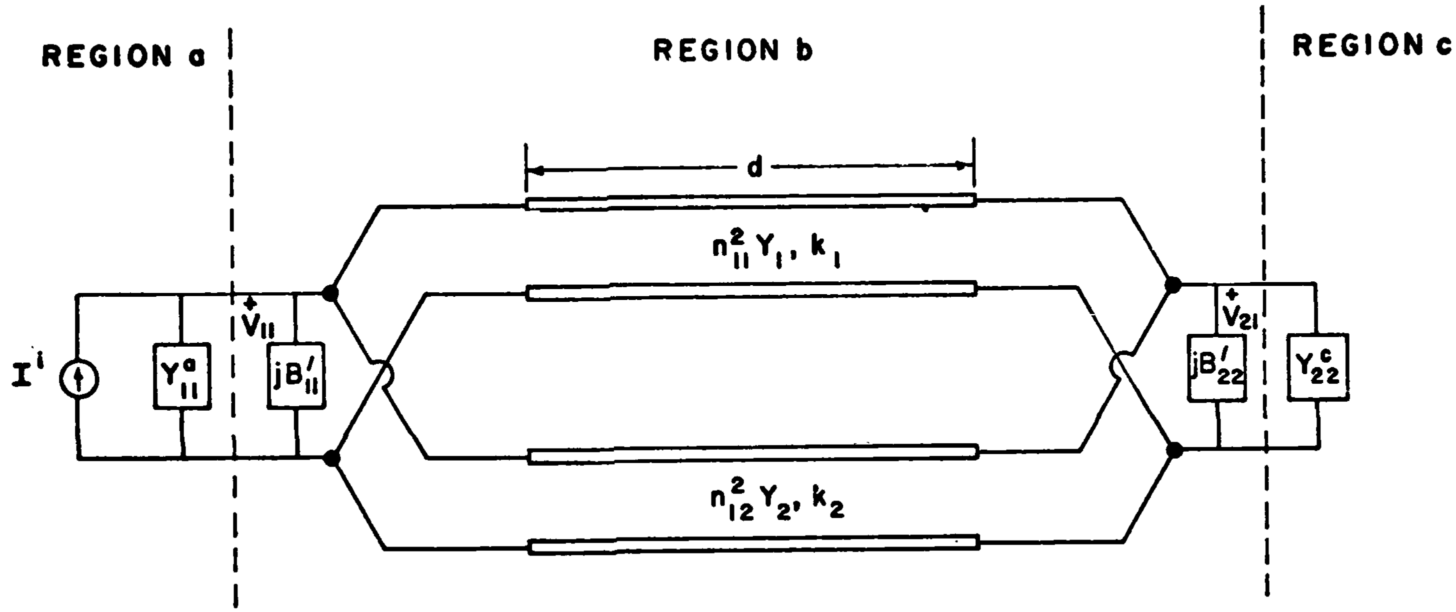

Fig. 10. Reduced representation of the equivalent circuit of Fig. 9 obtained by using $n_{21} = n_{11}$ and $n_{22} = n_{12}$.

The parameters related to the TE_{11} $(i = 1)$ and TM_{11} $(i = 2)$ modes should be specified. The normalized magnetic and electric field vectors of the TE_{11} mode in a cylindrical coordinate system, as given by (38) and (39), are

$$\underline{h}_1 = -0.887\left[\frac{1.841}{a} J_1'\left(\frac{1.841}{a}\rho\right) \sin\phi\, \underline{u}_\rho + \frac{1}{\rho} J_1\left(\frac{1.841}{a}\rho\right) \cos\phi\, \underline{u}_\phi\right] \tag{80}$$

$$\underline{e}_1 = \underline{h}_1 \times \underline{u}_z \tag{81}$$

Its modal wave number, as given by (40), is

$$k_1 = \left[\omega^2 \mu_b \varepsilon_b - \left(\frac{1.841}{a}\right)^2\right]^{1/2} \tag{82}$$

and its modal characteristic admittance, as given by (41), is

$$Y_1 = \frac{k_1}{\omega \mu_b} \tag{83}$$

The normalized magnetic and electric field vectors of the TM_{11} mode in a cylindrical coodinate system are [1, Sec. 8-1]

$$\underline{h}_2 = -0.517\left[\frac{1}{\rho} J_1\left(\frac{3.832}{a}\rho\right) \sin\phi\, \underline{u}_\rho + \frac{3.832}{a} J_1'\left(\frac{3.832}{a}\rho\right) \cos\phi\, \underline{u}_\phi\right] \tag{84}$$

$$\underline{e}_2 = \underline{h}_2 \times \underline{u}_z \tag{85}$$

Its modal wave number is

$$k_2 = \left[\omega^2 \mu_b \varepsilon_b - \left(\frac{3.832}{a}\right)^2\right]^{1/2} \tag{86}$$

and its modal characteristic admittance is

$$Y_2 = \frac{\omega\varepsilon_b}{k_2} \tag{87}$$

Other parameters of interest are the modal voltages $V_{111}(0)$ and $V_{112}(0)$. Substituting (80) and (84) in (23), one obtains

$$V_{111}(0) = \frac{0.816}{a} \tag{88}$$

$$V_{112}(0) = \frac{0.991}{a} \tag{89}$$

Now, the turns ratios n_{11} and n_{12} are readily determined from (88) and (89) by (78). We have

$$n_{11} = \frac{0.816}{a} \tag{90}$$

$$n_{12} = \frac{0.991}{a} \tag{91}$$

VIII. RESULTS AND CONCLUSIONS

The transfer admittance Y_{12} as given by (34) and the transmission cross section as given by (63) for normal incidence and one propagating mode in the cylindrical cavity were calculated and selected results are presented and discussed below. In the following explanations of results, an effort is made to outline how quantities of interest depend upon electrical dimensions of the aperture-cavity-aperture problem, to examine the effects of different dielectrics in the cavity region b and in the half-space region c, and to look at the effects of lossy material filling the cavity. Also, the influence of oblique incidence (TE field) is mentioned. Finally, the case of two propagating modes in the cavity is considered and examined by a numerical example.

The case of normal incidence and one propagating mode in the cylindrical cavity is treated in Figs. 11-16. The parameters Y_{12}, the transfer admittance, and TA, the transmission cross section, are periodic functions in d, the depth of the cavity. Thus, for practical consideration, they are only plotted in the neighborhood of the first resonant thickness. The permeability of all regions is that of free space and the permittivity of the different regions is specified for the different cases. The apertures A_1 and A_2 are assumed to be identical (i.e. $R_1 = R_2$). Finally, from (40) and (86) one readily obtains that the TE_{11} mode is the only propagating mode provided

$$\frac{1.841}{2\pi} \left(\frac{\varepsilon_a}{\varepsilon_b}\right)^{1/2} \lambda_a < a < \frac{3.832}{2\pi} \left(\frac{\varepsilon_a}{\varepsilon_b}\right)^{1/2} \lambda_a \qquad (92)$$

The real and imaginary parts of Y_{12} are shown in Fig. 11 for $a = 0.5\,\lambda_a$ and for aperture radii of $0.03\,\lambda_a$, $0.05\,\lambda_a$, and $0.1\,\lambda_a$, where

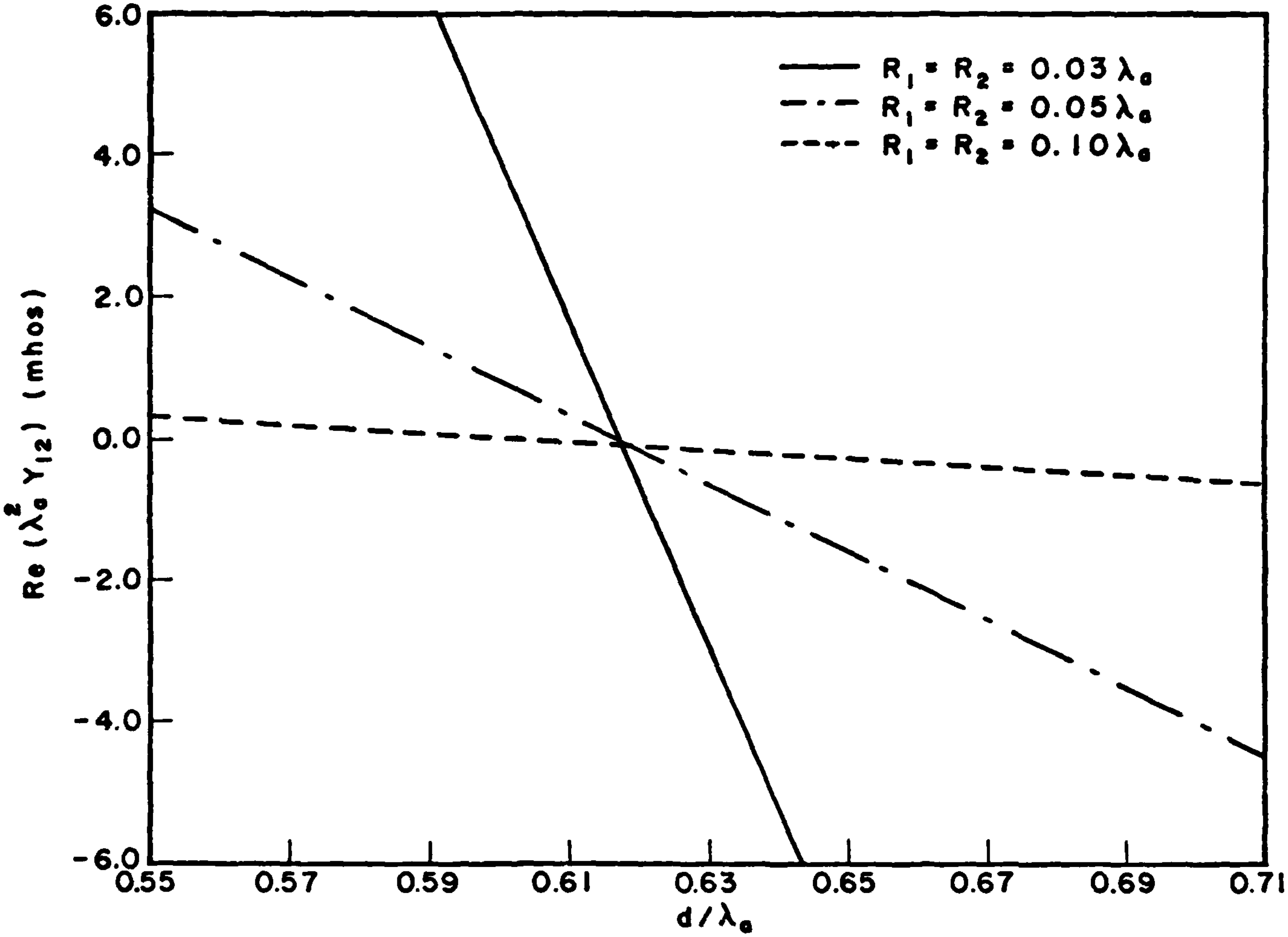

Fig. 11a. Plots of $Re(\lambda_a^2 Y_{12})$ versus d/λ_a for $\varepsilon_a = \varepsilon_b = \varepsilon_c = \varepsilon_o$, $a = 0.5\lambda_a$ with various radii R_1 and R_2. Cases shown are $R_1 = R_2 = 0.03\lambda_a$, $R_1 = R_2 = 0.05\lambda_a$, and $R_1 = R_2 = 0.10\lambda_a$.

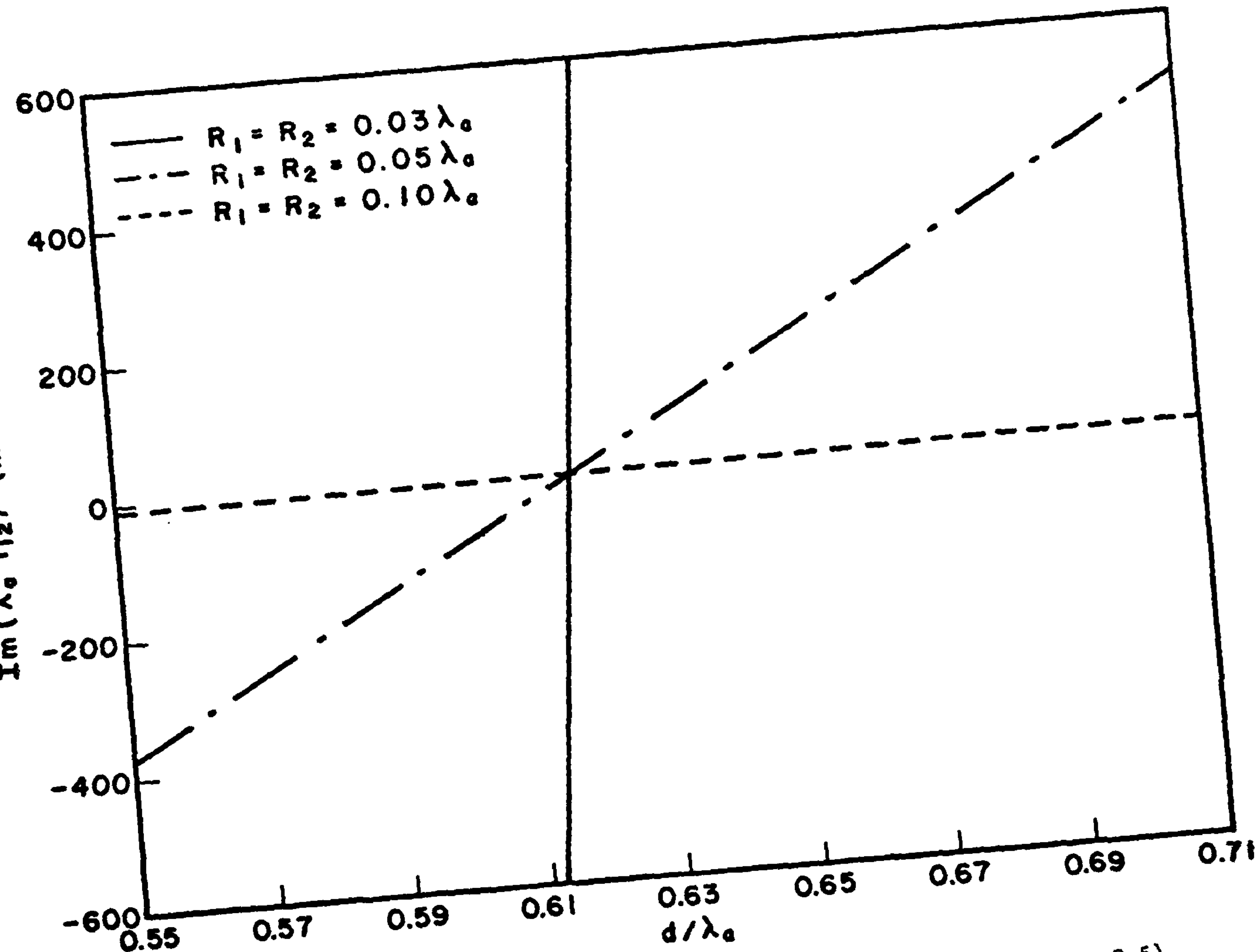

Fig. 11b. Plots of $Im(\lambda_a^2 Y_{12})$ versus d/λ_a for $\varepsilon_a = \varepsilon_b = \varepsilon_c = \varepsilon_o$, $a = 0.5\lambda_a$ with various radii R_1 and R_2. Cases shown are $R_1 = R_2 = 0.03\lambda_a$, $R_1 = R_2 = 0.05\lambda_a$, and $R_1 = R_2 = 0.10\lambda_a$.

λ_a is the wavelength in the half-space region a. As expected from (36) and (37), the imaginary part of Y_{12} becomes dominant as the apertures become electrically smaller.

The transmission cross sections (63) for the same problem are shown in Fig. 12. For electrically small apertures TA/λ_a^2 becomes a maximum, as predicted by (61), at so-called resonant depths, which approach $\lambda_1/2$, where $\lambda_1 = 1.234\lambda_a$ is the wavelength of the TE_{11} mode for $\varepsilon_b = \varepsilon_a$, $\mu_b = \mu_a$, and $a = 0.5\lambda_a$. The peak value of TA/λ_a^2 for all three cases is 10 log $(3/4\pi)$= -6.221 dB, which is the resonant result implied by (62).

When the cavity is loaded with different dielectrics the transmission resonances occur at cavity depths farther from $\lambda_1/2$, as given by (61). This fact is demonstrated for $a = 0.32\lambda_a$, $R_1 = R_2 = 0.05\lambda_a$ and $\varepsilon_a = \varepsilon_c = \varepsilon_o$ and $\varepsilon_b = \varepsilon_o$, $2\varepsilon_o$, and $3\varepsilon_o$ in Fig. 13a, Fig. 13b and Fig. 13c, respectively. Note that $\lambda_1 = 2.489\lambda_a$, $0.928\lambda_a$, and $0.680\lambda_a$ for the cases of $\varepsilon_b = \varepsilon_o$, $2\varepsilon_o$, and $3\varepsilon_o$ and thus the resonance actually occurs at different cavity depths measured in wavelengths in the half-space region a. The choice of the cylindrical cavity radius $a = 0.32\lambda_a$ ensures one propagating mode in all three cases. As the material filling the cavity becomes more dense, the transmission resonances become wider. For instance, the variation in d for which the transmission cross section is not less than -60 dB are $0.996\, d_{res} < d < 1.004\, d_{res}$, $0.990\, d_{res} < d < 1.010\, d_{res}$, and $0.987\, d_{res} < d < 1.014\, d_{res}$ for $\varepsilon_b = \varepsilon_o$, $\varepsilon_b = 2\varepsilon_o$ and $\varepsilon_b = 3\varepsilon_o$, respectively. Note that the magnitudes of the peaks, however, are constant. This result is, of course, in agreement with (58) which is independent of ε_b.

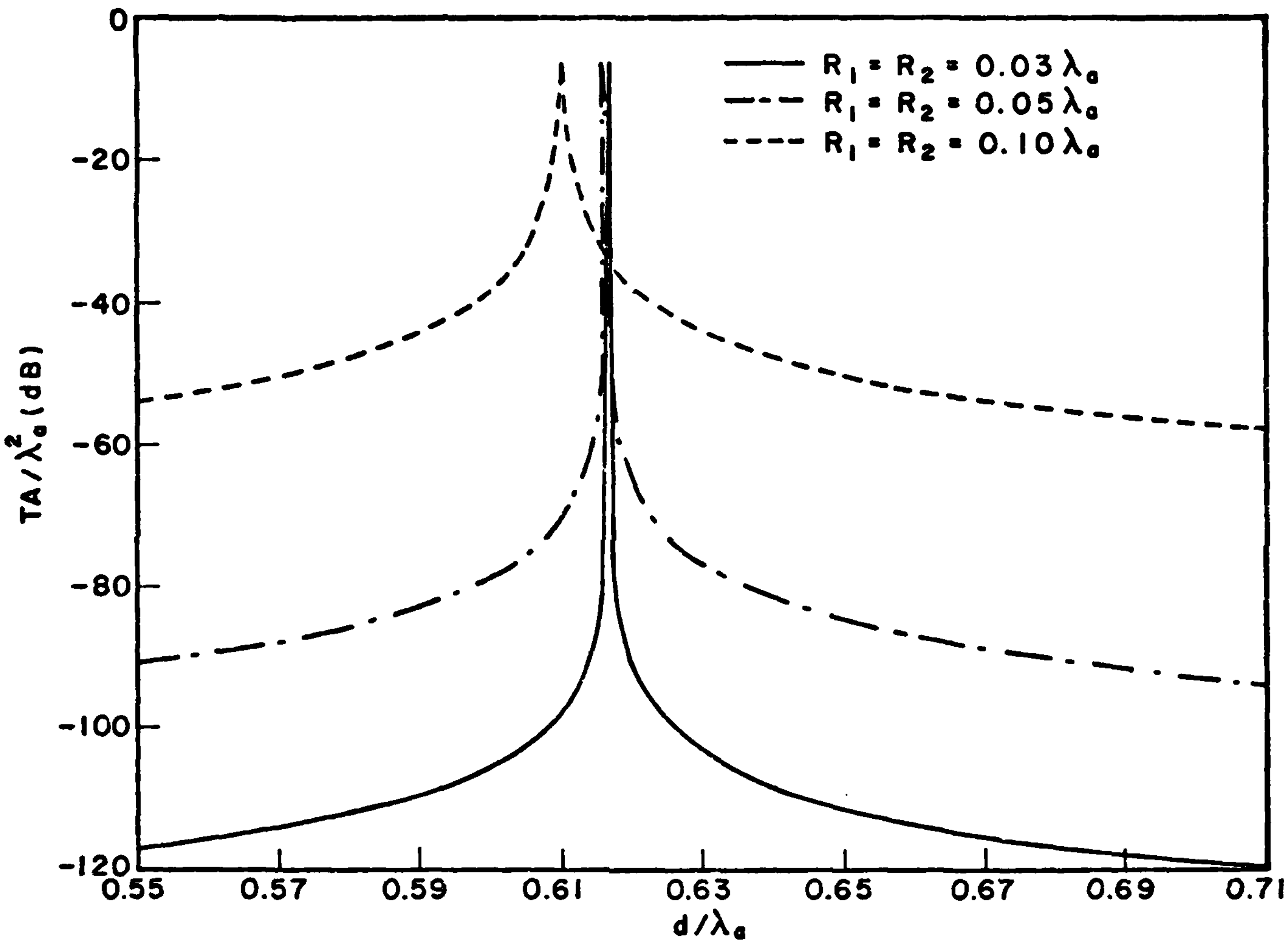

Fig. 12. Plots of transmission cross section versus d/λ_a for the case of Fig. 11. Cases shown are $R_1 = R_2 = 0.03\lambda_a$, $R_1 = R_2 = 0.05\lambda_a$, and $R_1 = R_2 = 0.10\lambda_a$.

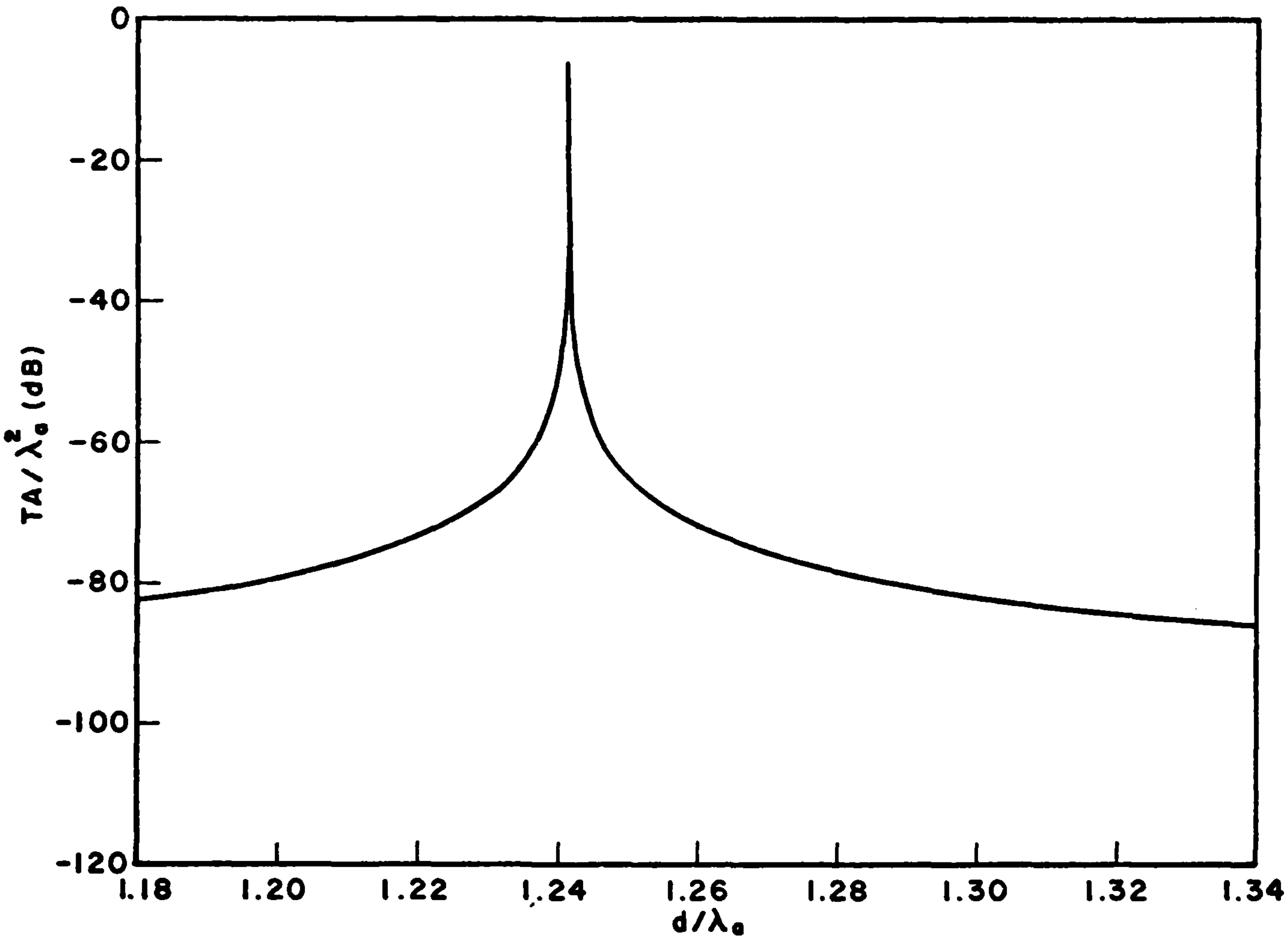

Fig. 13a. Plot of transmission cross section versus d/λ_a for $\varepsilon_a = \varepsilon_c = \varepsilon_o$, $a = 0.32\lambda_a$, $R_1 = R_2 = 0.05\lambda_a$ with $\dot{\varepsilon}_b = \varepsilon_o$.

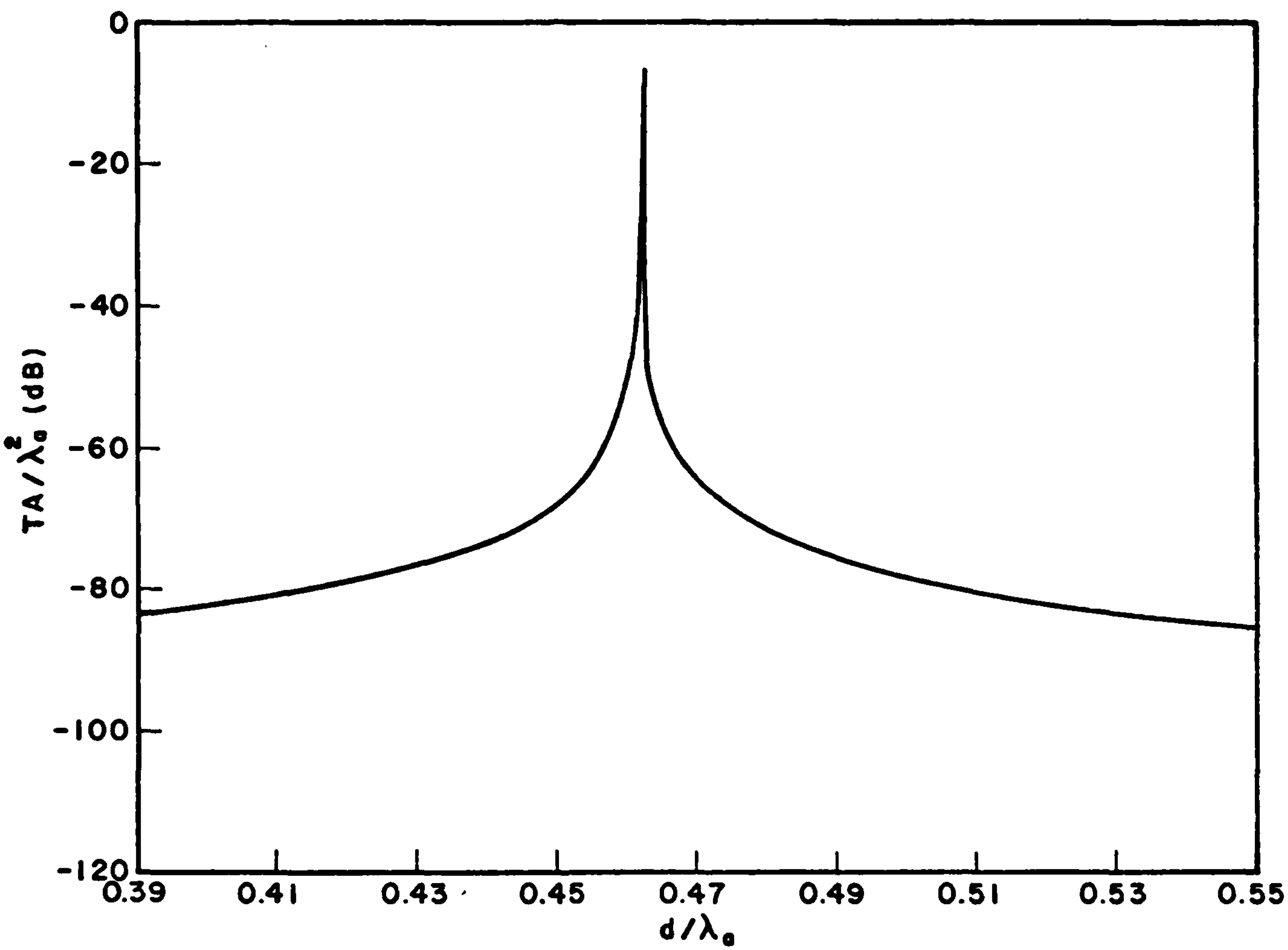

Fig. 13b. Plot of transmission cross section versus d/λ_a for $\varepsilon_a = \varepsilon_c = \varepsilon_o$, $a = 0.32\lambda_a$, $R_1 = R_2 = 0.05\lambda_a$ with $\varepsilon_b = 2\varepsilon_o$.

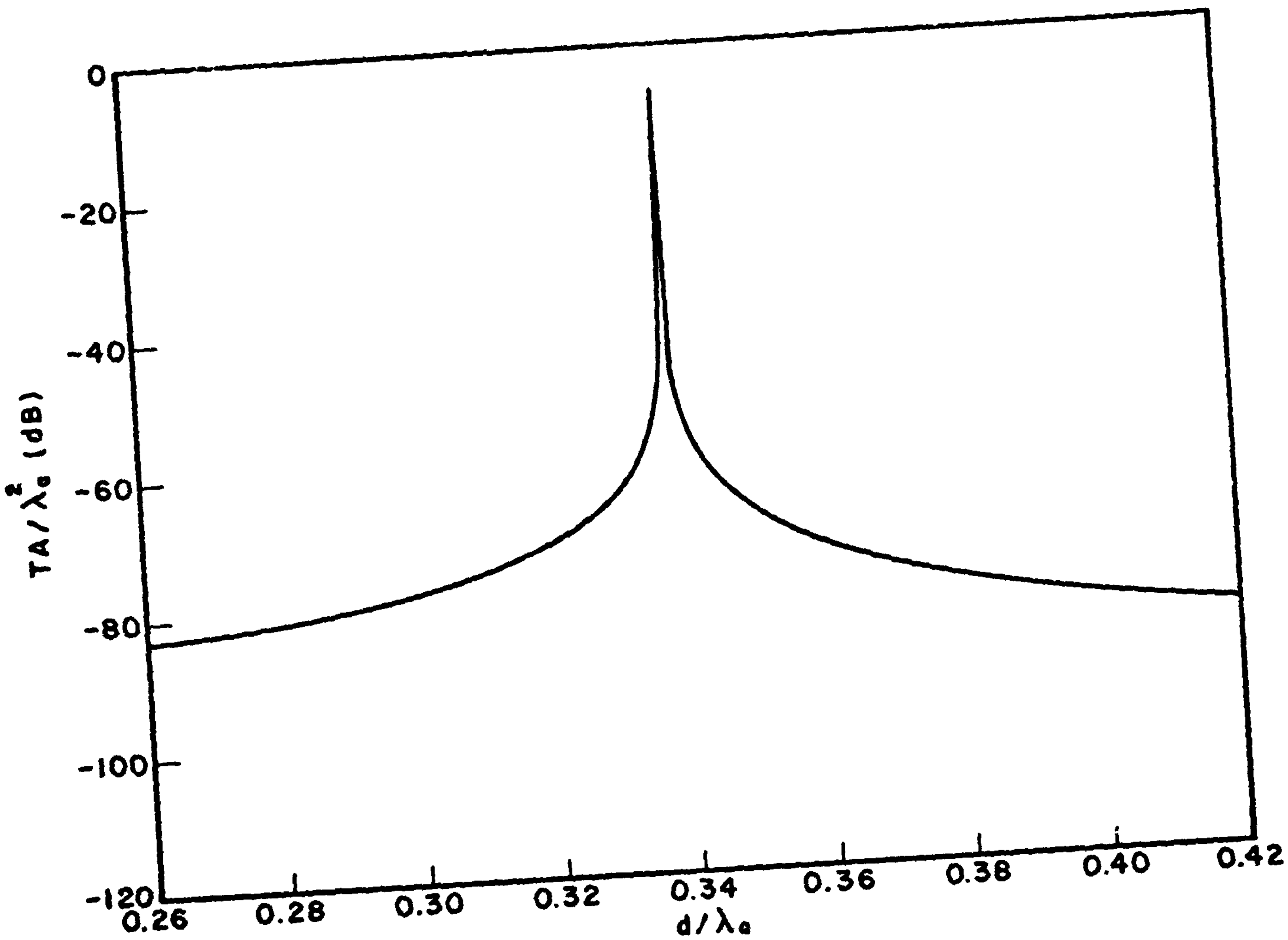

Fig. 13c. Plot of transmission cross section versus d/λ_a for $\varepsilon_a = \varepsilon_c = \varepsilon_o$, $a = 0.32\lambda_a$, $R_1 = R_2 = 0.05\lambda_a$ with $\varepsilon_b = 3\varepsilon_o$.

The effects of a different dielectric filling the half-space region c are depicted in Fig. 14. Here the cavity radius is $a = 0.5\lambda_a$, and the radii of the apertures are $R_1 = R_2 = 0.05\lambda_a$. As expected from (59), the position of the resonance condition is not a function of ε_c, and therefore is not affected. The peak values of the transmission cross section, however, decay in magnitude as ε_c becomes larger. The result is in agreement with (57) and (58) which reduce here ($\bar{\mu}_b = \bar{\mu}_c = 1$ and $\chi = 1$) to

$$\mathrm{Re}(Y_{12})_{res} = (-1)^{m+1} \frac{4\pi}{3\eta_a\lambda_a^2}(1 + \bar{\varepsilon}_c^{\,3/2}) \tag{93}$$

$$T_{res} = \frac{3\bar{\varepsilon}_c^{\,3/2}\lambda_a^2}{[1 + \bar{\varepsilon}_c^{\,3/2}]^2\,\pi A} \tag{94}$$

where $\bar{\varepsilon}_c = \varepsilon_c/\varepsilon_a$ as defined by (53).

If the dielectric filling the cavity is lossy, the expected decrease in the transmission cross section peaks is seen in Fig. 15, which presents the lossless case $\varepsilon_b = \varepsilon_o$, the lossy case $\varepsilon_b = (1 - j0.001)\varepsilon_o$, that is, with Q factor = 1000, and the lossy case $\varepsilon_b = (1 - j0.01)\varepsilon_o$, that is, with Q factor = 100. Here the cavity radius is $a = 0.5\lambda_a$. Note that the loss does not affect the position of the resonances. The real and imaginary parts of Y_{12} for this case are shown in Fig. 16. As may be observed, the loss does not affect the imaginary part of Y_{12}. In contrast, its real part has changed significantly. $\mathrm{Re}(\lambda_a^2 Y_{12})$ for the case $\varepsilon_b = (1 - j0.01)\varepsilon_o$ could not be shown in Fig. 16a since it varies between 19 and 29 mhos.

If the two apertures are of different size, i.e., $R_1 \neq R_2$, (57) and (58), for the case of three similar media (i.e., $\bar{\mu}_b = \bar{\mu}_c = \bar{\varepsilon}_c = 1$), reduce, respectively, to

$$\mathrm{Re}(Y_{12})_{res} = (-1)^m \frac{4\pi}{3\eta_a\lambda_a^2}\left[2 - (1 + \chi)(1 + \frac{1}{\chi})\right] \tag{95}$$

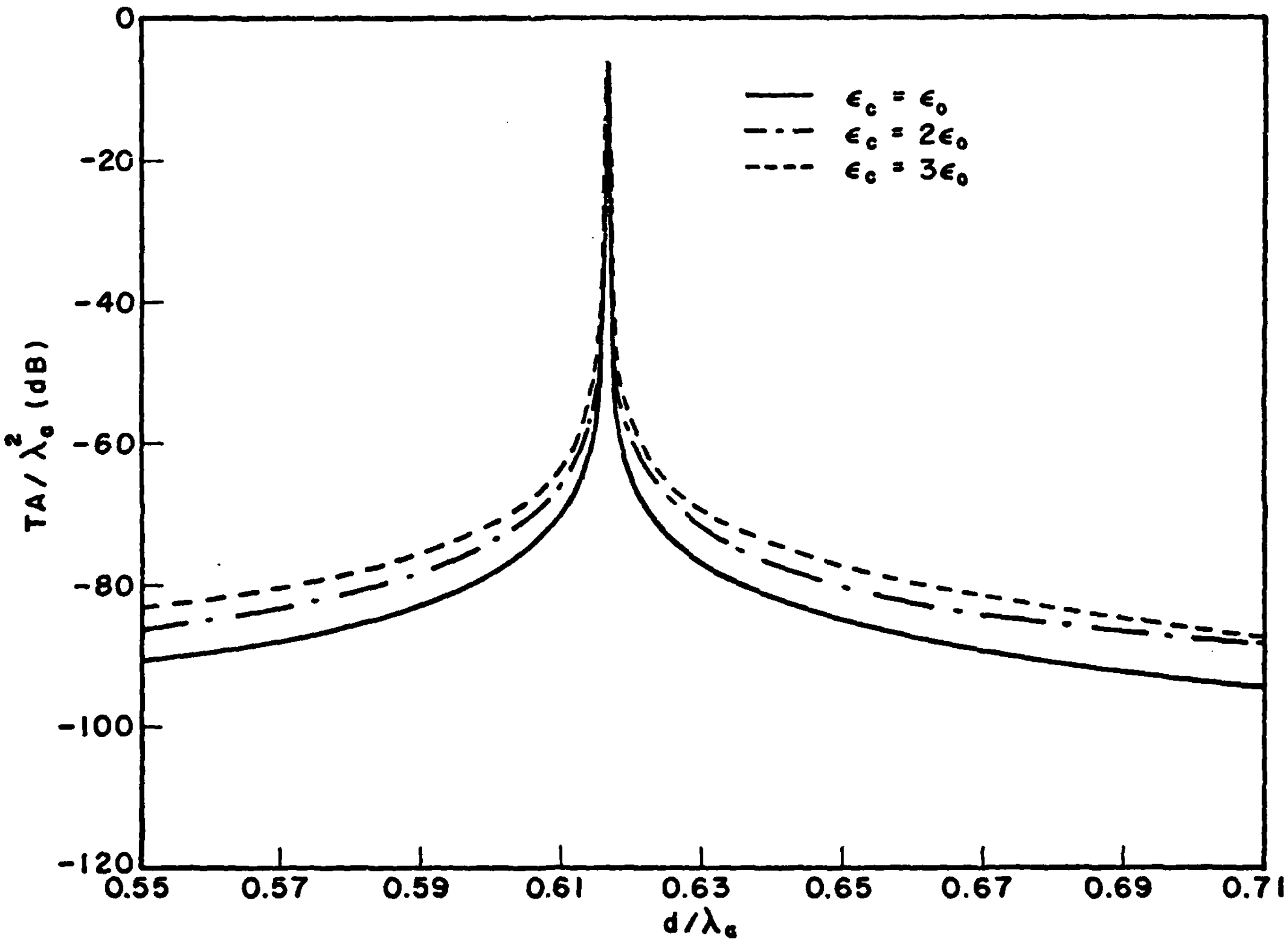

Fig. 14. Plots of transmission cross section versus d/λ_a for $\varepsilon_a = \varepsilon_b = \varepsilon_o$, $a = 0.5\lambda_a$, $R_1 = R_2 = 0.05\lambda_a$ and different dielectrics in region c. Cases shown are $\varepsilon_c = \varepsilon_o$, $\varepsilon_c = 2\varepsilon_o$, and $\varepsilon_c = 3\varepsilon_o$.

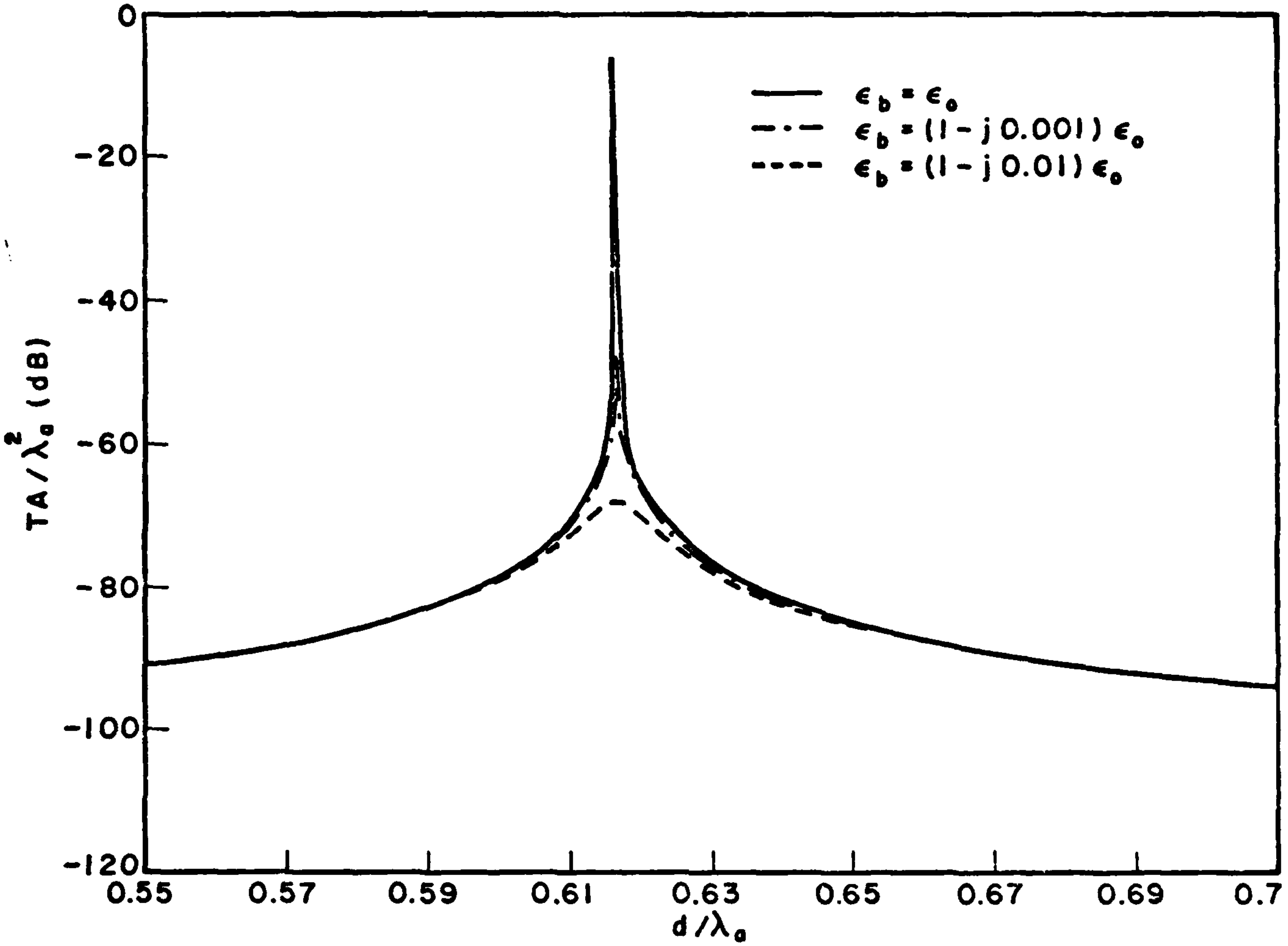

Fig. 15. Plots of transmission cross section versus d/λ_a for $\varepsilon_a = \varepsilon_c = \varepsilon_o$, $a = 0.5\lambda_a$, $R_1 = R_2 = 0.05\lambda_a$ for lossy dielectric in cavity. Cases shown are $\varepsilon_b = \varepsilon_o$, $\varepsilon_b = (1 - j0.001)\varepsilon_o$, and $\varepsilon_b = (1 - j0.01)\varepsilon_o$.

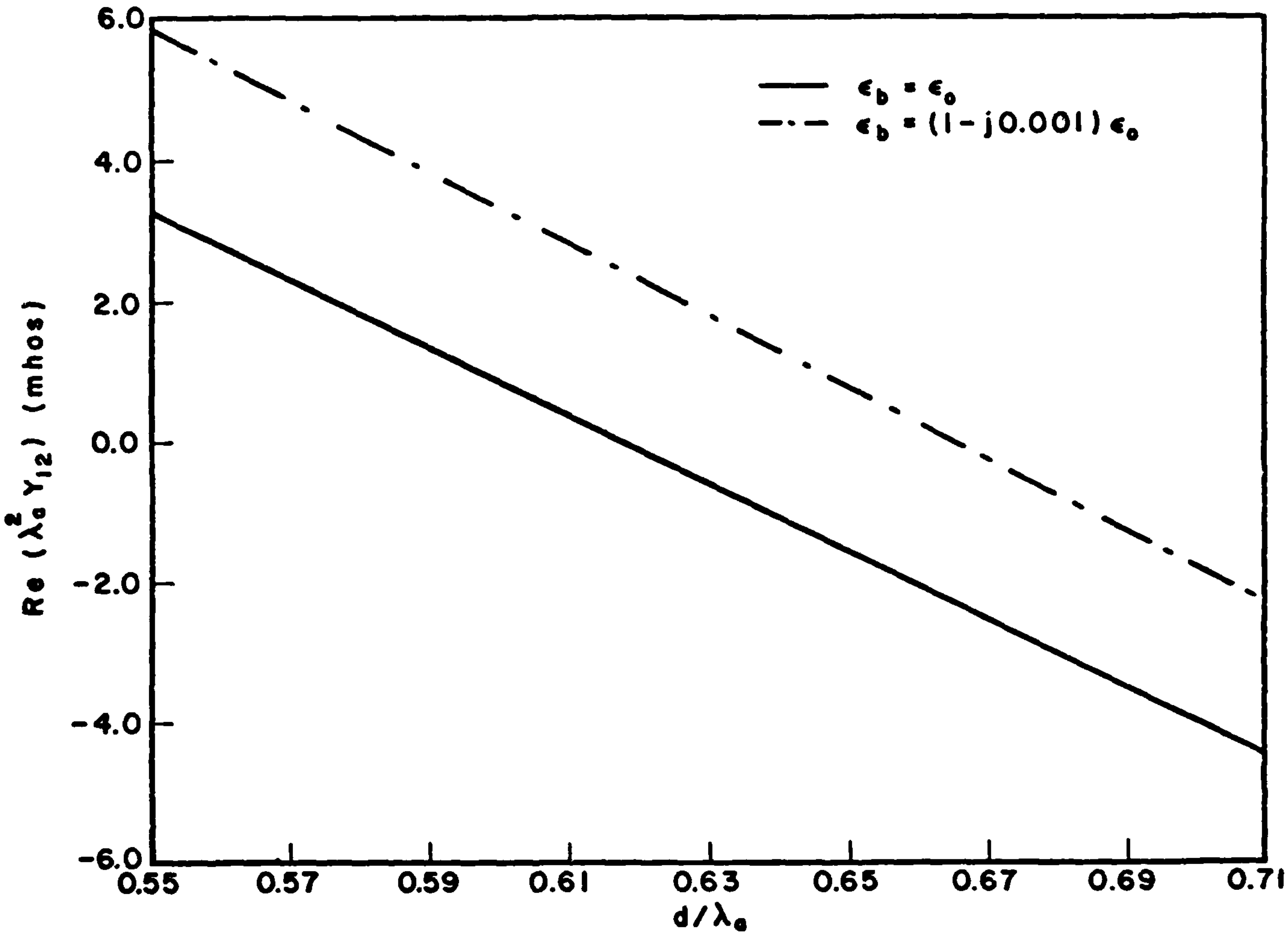

Fig. 16a. Plots of $Re(\lambda_a^2 Y_{12})$ versus d/λ_a for the case of Fig. 15. Cases shown are $\varepsilon_b = \varepsilon_o$, and $\varepsilon_b = (1 - j0.001)\varepsilon_o$.

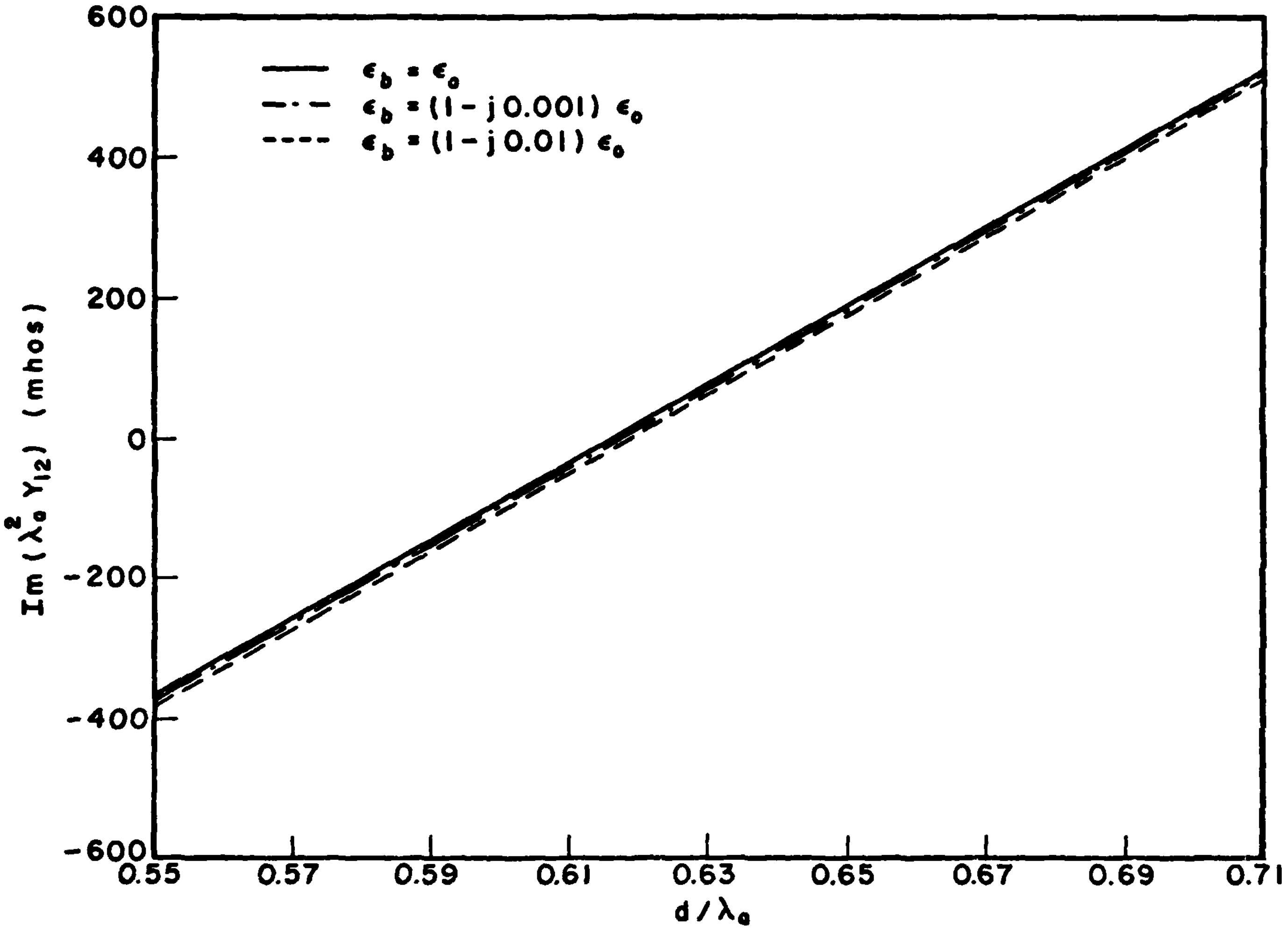

Fig. 16b. Plots of $\mathrm{Im}(\lambda_a^2 Y_{12})$ versus d/λ_a for the case of Fig. 15. Cases shown are $\varepsilon_b = \varepsilon_o$, $\varepsilon_b = (1 - j0.001)\varepsilon_o$, and $\varepsilon_b = (1 - j0.01)\varepsilon_o$.

$$T_{res} = \frac{3\lambda_a^2}{\pi[2 - (1 + \chi)(1 + \frac{1}{\chi})]^2 A} \tag{96}$$

From (96) one can easily show that T_{res} is maximum when $\chi = 1$, that is when the two apertures are identical. This is in agreement with the fact that when $R_1 = R_2$ the power transmitted, at resonance, is equal to the maximum power that can be delivered to a load by the source and its internal admittance $Y_{11}^a + jB_{11}$ in Fig. 7.

The effect of TE (transverse electric to the cylinder axis) oblique incidence is shifting the transmission cross section graphs down by $10 \log(\cos^2 \theta_{inc})$ decibels, where θ_{inc}, the angle of incidence, is shown in Fig. 8. Otherwise, TE oblique incidence is the same as TEM normal incidence. Hence, no further detail regarding TE oblique incidence is necessary.

Finally, the case of normal incidence and two propagating modes in the cylindrical cavity is treated in Fig. 17. The permeability and permittivity of all regions are those of free space. The apertures A_1 and A_2 are identical and $R_1 = R_2 = 0.05\lambda_a$. From (86) and the fact that the wave number of the third mode, the TE_{12} mode, is

$$k_3 = [\omega^2\mu_b\varepsilon_b - (\frac{5.331}{a})^2]^{1/2} \tag{97}$$

one readily obtains that the TE_{11} and TM_{11} modes are the only propagating modes provided

$$\frac{3.832}{2\pi} (\frac{\varepsilon_a}{\varepsilon_b})^{1/2} \lambda_a < a < \frac{5.331}{2\pi} (\frac{\varepsilon_a}{\varepsilon_b})^{1/2} \lambda_a \tag{98}$$

Accordingly, the cavity radius is taken to be $a = 0.75\lambda_a$.

The transmission cross section in Fig. 17 is plotted in the neighborhood of the first two resonant depths. The transmission cross section peaks are located at these depths, which approach, respectively, $\lambda_1/2$

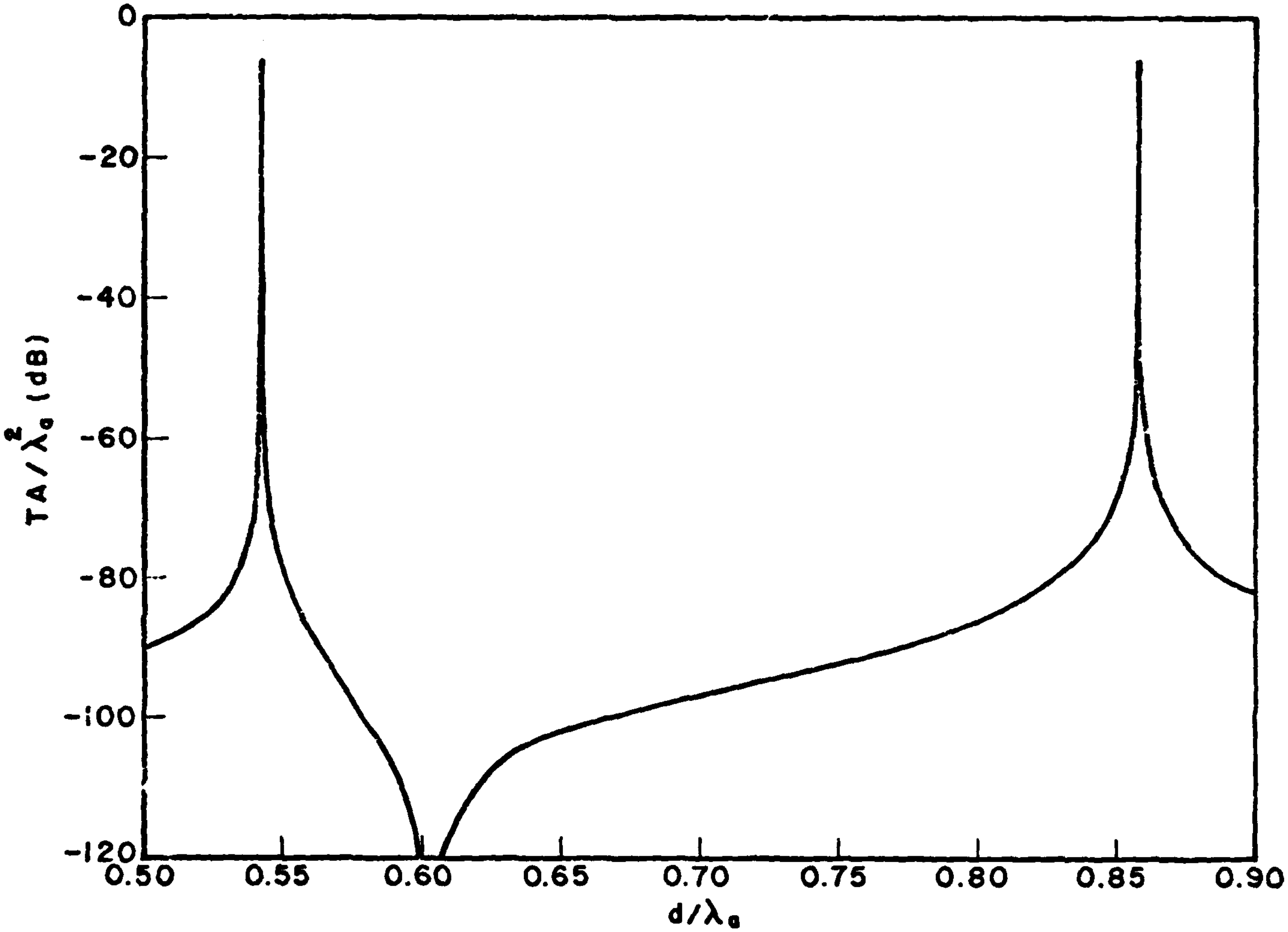

Fig. 17. Plots of transmission cross section versus d/λ_a for $\varepsilon_a = \varepsilon_b = \varepsilon_c = \varepsilon_o$, $a = 0.75\lambda_a$, and $R_1 = R_2 = 0.05\lambda_a$ for the case of two propagating modes in the cavity.

and $\lambda_2/2$, where $\lambda_1 = 1.086\lambda_a$ is the wavelength of the TE_{11} mode and $\lambda_2 = 1.718\lambda_a$ is the wavelength of the TM_{11} mode. The magnitude of the two peaks is the same and equal to -6.221 dB, which is the peak value obtained when only one mode was propagating.

IX. DISCUSSION

Electromagnetic coupling between two half-space regions through an aperture to cavity to aperture system has been investigated and a simple equivalent circuit has been developed for the special case of a circular cylindrical cavity with a small circular aperture centered in each of its end faces. It was found that for certain cavity depths the system becomes resonant, thereby increasing by orders of magnitude the power transmitted by the aperture to cavity to aperture system over what it would transmit for other cavity depths.

It should be emphasized that, if the generalized concept of small-aperture polarizability which adds a radiation conductance term to the aperture admittance had not been used, infinities in the aperture fields and power transmitted would have occurred.

The result that, at resonances, the transmission cross section of the coupling system is independent of the size of the apertures (provided $R_1 = R_2$) is to be expected because similar results have been obtained for other transmission and scattering problems. For example, the transmission width of a narrow infinitely long slot in a thick conductor at resonance is $\frac{\lambda}{\pi}$, regardless of its actual width [4]. Moreover, the transmission cross section obtained here is the same as that obtained in [7] for a small slot in a zero-thickness plane conducting screen resonated by a capacitor placed across its midpoint.

The preceding paragraph applies only to ideal loss-free problems. Dielectric and conductor losses can significantly decrease the transmission cross section at resonance. This decrease has been demonstrated via numerical examples.

REFERENCES

[1] R. F. Harrington, Time Harmonic Electromagnetic Fields, McGraw-Hill Book Co. , 1961.

[2] R. F. Harrington, Field Computation by Moment Methods, Macmillan Company, 1968.

[3] R. F. Harrington and J. R. Mautz, "A Generalized Network Formulation for Aperture Problems," IEEE Trans. Antennas Propagate., vol. AP-24, No. 6, pp. 870-873, November 1976.

[4] R. F. Harrington and D. T. Auckland, "Electromagnetic Transmission Through Narrow Slots in Thick Conducting Screens," IEEE Trans.Antenna Propagate., vol. AP-28, No. 5, pp. 616-622, September 1980.

[5] H. A. Bethe, "Theory of Diffraction by Small Holes," Phys. Rev., vol. 66, pp. 163-182, October 1944.

[6] C. J. Bouwkamp, "On Bethe's Theory of Diffraction by Small Holes," Philips Res. Rep., vol. 5, pp. 321-332, October 1950.

[7] R. F. Harrington, "Resonant Behavior of a Small Aperture Backed by a Conducting Body," IEEE Trans. Antennas Propagate., (to be published).

[8] R. F. Harrington, "Cavity-backed Apertures,"Lecture Notes for Short Course on Computational Methods in Electromagnetics, St. Cloud, Florida, Nov. 1980.

[9] C. M. Butler, "Investigation of a Scatterer Coupled to an Aperture in a Conducting Screen," IEE Proc., vol. 127, pt. H, no. 3, pp. 161-169, June 1980.

[10] N. A. McDonald, "Electric and Magnetic Coupling through Small Apertures in Shield Walls of any Thickness," IEEE Trans. Microwave Theory Tech., vol. MTT-20, No. 10, pp. 689-695, October 1972.

MISSION
of
Rome Air Development Center

RADC plans and executes research, development, test and selected acquisition programs in support of Command, Control Communications and Intelligence (C^3I) activities. Technical and engineering support within areas of technical competence is provided to ESD Program Offices (POs) and other ESD elements. The principal technical mission areas are communications, electromagnetic guidance and control, surveillance of ground and aerospace objects, intelligence data collection and handling, information system technology, ionospheric propagation, solid state sciences, microwave physics and electronic reliability, maintainability and compatibility.